Desalination and Water Treatment
www.deswater.com

doi: 10.1080/19443994.2013.822187

52 (2014) 6567–6590
October

Taylor & Francis
Taylor & Francis Group

TiO_2 photocatalysis: progress from fundamentals to modification technology

P. Pattanaik[a,]*, M.K. Sahoo[b,]*

[a]*Department of Chemistry, Government College, Angul 759 122, India*
Tel. +91 9437059431; email: pattanaikpranayini@gmail.com
[b]*Department of Chemistry, North-Eastern Hill University, Shillong 793 022, India*
Tel. +91 364 2722632; Fax: +91 364 2551634; email: mksahoo@nehu.ac.in

Received 2 August 2012; Accepted 18 June 2013

ABSTRACT

Heterogeneous photocatalysis is a promising method among advanced oxidation processes, which can be used for degradation of various organic pollutants in water and air. In heterogeneous photocatalysis, illumination of an oxide semiconductor, usually the anatage form of titanium dioxide, by UV radiation produces photo-excited electrons (e^-) and positively charged holes (h^+). In the aqueous phase, the illuminated surface is extensively regarded as a producer of hydroxyl radicals ($h^+ + OH^- = HO^\bullet$). These hydroxyl radicals, holes, and conduction-band electrons can degrade organic pollutants directly or indirectly. However, the massive recombination of these photo-generated charge carriers and large band gap of TiO_2 limits its overall photocatalytic efficiency. These limitations can be overcome by changing surface properties of titania by adding suitable electron scavengers in the reaction medium or by modifying its electronic band structure through strategies like metal ion/nonmetal atom doping, narrow band-gap semiconductor coupling, sensitization by organic dyes, etc. Based on recent studies reported in the literature, nonmetal ion doping and dye sensitization are very effective methods to extend the activating spectrum to visible radiation. This review emphasizes on the visible-light activation of TiO_2 and its application to environmental remediation.

Keywords: Heterogeneous photocatalysis; Mineralization; Doping; Dye sensitization; Composite semiconductor

1. Introduction

Heterogeneously dispersed semiconductor surfaces are advantageous to provide chemical environment to a wide range of adsorbates and means to initiate light-induced redox reaction in these weakly associated adsorbates. Upon photoexcitation of several semiconductors, heterogeneously suspended, either in aqueous or nonaqueous medium, simultaneous oxidation and reduction reactions occur. This conversion accomplishes complete oxidative degradation of an organic substrate present in the system. Molecular oxygen may act like an oxidizing agent in a few gas or solid phase reactions. The incident light that initiates the reaction is in the visible or low range of UV region of spectrum. It is absorbed by the heterogeneously dispersed particulate semiconductor leading to photoactivation. During the process, photo-induced

---

*Corresponding authors.

molecular transformations or reactions take place at the surface of the catalyst.

In heterogeneous photocatalysis, two or more phases are used and a light source with a semiconductor material is used to initiate the photoreaction. UV light of long wavelength or even sunlight can be used. This is possibly the best method to remove organic species in the environment [1]. Because, the process gradually breaks down the contaminant molecule and no residue of the original material remains. The catalyst itself remains unchanged during the process and no consumable chemicals are required. Moreover, the contaminant is attracted strongly to the surface of the catalyst, so the process works at very low concentrations. The major factors affecting the process are: initial organic contaminants (OCs), amount of catalyst, irradiation time, presence of ions [2], temperature [3], solution's pH [4], and light intensity [5].

The discovery of photocatalytic splitting of water on electrodes by Fujishima and Honda [6] marked the beginning of a new era in heterogeneous photocatalysis. Since then, efforts in understanding the fundamental processes of semiconductor photocatalysis and enhancing its efficiency have gained momentum. In recent years, applications to environmental clean-up have become most active areas in heterogeneous photocatalysis. The potential application of TiO_2-based photocatalysis aims at the total destruction of organic compounds (OCs) in polluted air and wastewater [7,8]. It has been used successfully for the mineralization of a wide variety of compounds such as alkanes, alcohols, carboxylic acids, alkenes, phenols [9], simple aromatics, halogenated hydrocarbons, surfactants, pharmaceuticals [10,11], and pesticides [12,13] as well as dyes from textile industry wastewater [14–16]. Photocatalysis has also been extended to water-splitting technology to produce solar hydrogen to support the future hydrogen economy [17]. A novel photo-induced super hydrophilic phenomenon involving TiO_2 has also been reported [18].

The whole discussion is divided into three parts. In the first part, conventional photocatalysis and its fundamentals have been discussed. In the second part, the recent trend of using modified titanium dioxide and the formulation of simplified mechanism of modification technologies have been described. Modified titanium dioxide is efficient for the photocatalytic degradation of pollutants under visible-light irradiation. In the third part, important applications of photocatalysis have been discussed. Photocatalytic mineralizations of contaminants present in water and air and production of hydrogen from water splitting utilizing TiO_2 have been discussed to show novel applications of semiconductor photocatalysis.

2. Fundamentals of photocatalysis

2.1. Photocatalytic materials

Solids that can promote reactions in the presence of light and are not consumed in the overall reaction are referred to as heterogeneous photocatalysts. These are invariably semiconductors. An ideal photocatalyst for photocatalytic oxidation (PCO) is characterized by the following attributes [19]:

- Photo-stability (i.e. not prone to photocorrosion);
- Photo-activity and photo-suitability towards visible or near UV light;
- Chemical and biological inertness;
- Availability and low cost;
- Nontoxicity; and
- Capability to adsorb reactants under efficient photonic activation.

Many semiconductors such as TiO_2, ZnO, ZrO_2, CdS, MoS_2, Fe_2O_3, CdS, SnO_2, ZnS, WO_3, etc. have been examined and used as photocatalysts for the degradation of OCs [20,21]. In nature, TiO_2 crystallizes into three polymorphs: anatase, rutile, and brookite. Anatase is thermodynamically less stable than rutile and exhibits a shorter wavelength absorption edge. Frequently present in nano-sized TiO_2 particles, it is largely recognized to be the most active agent in the oxidative detoxification reactions. TiO_2 is one of the most efficient catalysts for the production of hydrogen and oxygen from water in the presence of UV-part of solar light [22,23]. Among the semiconductor photocatalysts available, TiO_2 is the most extensively studied photocatalyst owing to its properties like resistance to photocorrosion, low cost, ready availability, nontoxicity, and its applicability at ambient conditions. Of the three common TiO_2 crystalline forms, anatase and rutile forms have been investigated extensively as photocatalysts. Anatase is reported to be more active as a photocatalyst than rutile. Evonik Degussa P25 is a titania photocatalyst that is used widely because of its high-level photocatalytic activity. It is composed of anatase and rutile crystallites; the reported ratio is 70:30 or 80:20 without being sure of its actual composition. In a typical analysis, crystalline composition of P25 was evaluated to be 78% anatase and 14% rutile. Assuming the remaining 8% part corresponds to amorphous phase, the anatase–rutile–amorphous ratio is determined to be 78:14:8 [24]. The minimum band-gap energy required for a photon to cause photogeneration of charge carriers over the TiO_2 semiconductor (anatase form) is 3.2 eV corresponding to a wavelength of less than 400 nm [25]. Actually, photoactivation in TiO_2 takes place in the range 300–380 nm. The minimum wavelength required to promote an electron depends upon the band-gap energy of the photocatalyst (Eq. (1)) as suggested by Mills et al. [26]. The band-gap energy of various photocatalysts [20,21] is listed in Table 1. Numerous studies on the application of PCO for the removal and mineralization of organic pollutants [3,26–31] in aqueous solutions have been reported.

$$E_{bg} = \frac{1,240}{\lambda_{\min}} \tag{1}$$

Due to the high band-gap energies of SnO_2 and ZnS, the light energy may not be sufficient to activate the catalyst. Catalysts like CdS and Fe_2O_3 have smaller band-gap energies [21]. The smaller band gap permits rapid recombination of hole and electron, and hence a negligible photocatalytic activity may be observed. However, due to the higher surface area of ZnO ($10\,m^2\,g^{-1}$) over TiO_2 (anatase, $8.9\,m^2\,g^{-1}$), ZnO may show greater photocatalytic activity than TiO_2. In accordance with the above facts, it has been reported that the dye Acid Red 18 (AR 18) undergoes maximum degradation with ZnO over TiO_2 (anatase) catalyst, while SnO_2, Fe_2O_3, CdS, and ZnS have negligible activity on AR18 decolorization and degradation [32]. But, ZnO suffers a major drawback in that it corrodes during the oxidation process. When ZnO suspensions are UV-irradiated, the valence-band (VB) holes that are photo-generated can thermodynamically oxidize the ZnO semiconductor because its decomposition potential is located within the band gap [33]. Some ZnO dissolves forming Zn^{2+} ions even in the dark on stirring the aqueous suspension owing to the amphoteric nature of this metal oxide. Further, the quantity of Zn^{2+} is seen to increase when irradiated with the 400-W lamp, relative to the 75-W light source [34]. In spite of this drawback, many other authors have attempted using ZnO in the PCO process [35–37]. Some other metal oxides including CeO_2, SnO_2, WO_2, and CdS have also been examined for OCs degradation [38–40].

Table 1
Band-gap energy of various photocatalysts

Photocatalyst	Band-gap energy (eV)	Photocatalyst	Band-gap energy (eV)
Si	1.10	ZnO	3.20
TiO_2 (rutile)	3.00	TiO_2 (anatase)	3.20
WO_3	2.70	CdS	2.40
ZnS	3.70	$SrTiO_3$	3.40
SnO_2	3.87	WSe_2	1.20
Fe_2O_3	2.20	$\alpha - Fe_2O_3$	3.10
SiC	3.00		

2.2. Principles of PCO process

In the PCO process, organic pollutants are destroyed in the presence of semiconductor photocatalysts (e.g. TiO_2 and ZnO), an energetic light source, and an oxidizing agent such as oxygen or air. As illustrated in Fig. 1, only photons with energies greater than the band-gap energy (E) can result in the excitation of VB electrons, which then promote the possible reactions with organic pollutants. The absorption of photons with energy lower than E or longer wavelengths usually causes energy dissipation in the form of heat. The illumination of the photocatalytic surface with sufficient energy ($\lambda \leqslant 380\,nm$ for TiO_2 and ZnO), leads to the formation of an electron-*hole pair: a positive hole in the VB and an electron in the conduction* band (e^-_{CB}) (Eq. (2)). The holes (h^+_{vb}) and electrons (e^-_{CB}) can either undergo recombination and dissipate the input energy as heat or migrate separately to the surface of TiO_2 particles, get trapped in metastable surface states, or react with electron donors and electron acceptors adsorbed on the semiconductor surface or within the surrounding electrical double layer of the charged particles.

In the absence of suitable electron and hole scavengers, the stored energy is dissipated within a

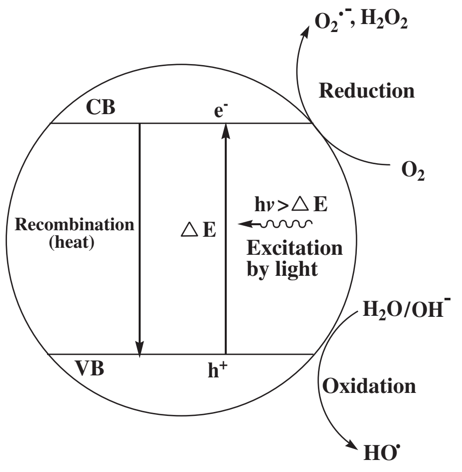

Fig. 1. Simplified mechanism of photocatalytic process showing photo-excited semiconductor to produce hydroxyl radical and superoxide radical anion from water and oxygen respectively.

few nanoseconds by recombination. If a suitable scavenger or surface defect is available to trap the electron or hole, recombination is prevented and subsequent redox reactions occur. The (h^+_{vb}), being a strong oxidant (+1.0 to + 3.5 V vs. NHE depending on the semiconductor and pH), either oxidizes the adsorbed organic substrates directly or reacts with electron donors like surface-bound water or hydroxide ions leading to the formation of adsorbed hydroxyl radical [41–43] within a few picoseconds, which is also a potent oxidizer (Eqs. (3)–(5)). The conduction-band electrons are good reductants (+0.5 to −1.5 V vs NHE) and they react with reducible species to prevent a build-up of charge. Thus, the (e^-_{CB}) reduces the oxygen adsorbed on the photocatalyst (TiO_2) to a superoxide anion radical, $O_2^{\cdot -}$ (Eq. (6)). We will see later that $O_2^{\cdot -}$ is involved in the generation of hydrogen peroxide (HP) and ultimately HO, which is involved in the degradation process (Eqs. (7)–(9)).

$$TiO_2 + h\nu \rightarrow e^-_{CB} + h^+_{vb} \tag{2}$$

$$h^+_{vb} + H_2O \rightarrow HO^{\cdot}_{surf} + H^+ \tag{3}$$

$$h^+_{vb} + HO^- \rightarrow HO^{\cdot}_{surf} \tag{4}$$

$$h^+_{vb} \text{ or } HO^{\cdot}_{surf} + \text{Organic molecule} \rightarrow \text{Intermediates} \rightarrow CO_2 + H_2O \tag{5}$$

$$e^-_{CB} + O_2 \rightarrow O_2^{\cdot -} \tag{6}$$

Photochemical oxidation may occur by either indirect oxidation via the surface-bound hydroxyl radical (i.e. a trapped hole at the particle surface) or directly via the valence-band hole before it is trapped either within the particle or at the particle surface. It is not possible to distinguish between a trapped hole and an adsorbed $HO^{\cdot}$ radical. It is suggested that adsorbed $HO^{\cdot}$ radical (or surface trapped h^+_{vb}) is the major oxidant while free $HO^{\cdot}$ radicals play only a minor role, if any [44]. The $HO^{\cdot}$ attacks a variety of OCs e.g. chlorinated aromatics, aniline, nitrophenols, etc., leading to various reaction intermediates depending on the nature of the compounds. The resulting intermediates further react with $HO^{\cdot}$ to produce final degradation products such as CO_2 and H_2O. In the photocatalytic degradation of pollutants, when the reduction process of oxygen and the oxidation of pollutants do not advance simultaneously, there is an electron accumulation in the CB, thereby causing an increase in the rate of recombination of e^-_{CB} and h^+_{vb} [3,43]. Thus, it is of paramount importance to prevent electron accumulation in an efficient PCO. Further, it is reported that the preferred oxidation route is highly compound-dependent. Those species that adsorb strongly to TiO_2 (highly polar compounds) are more likely to oxidize via the surface-trapped holes. The compounds which have no hydrogen atoms available for abstraction by OH radical are oxidized by VB holes. On the other hand, it is important for the excited electron in the conduction band to be scavenged by an external agent to prevent its recombination with the positive hole under ambient conditions, which otherwise would lead to very low quantum yields. Use of suitable electron scavengers or the presence of a surface defect state can trap the electron prolonging the lifetime of the hole.

In PCO, the catalyst can either provide energy levels to mediate electron transfer between adsorbate molecules (by temporarily accommodating an electron) or behave as both an electron donor (the photo-generated electron in the conduction band) and an electron acceptor (the photo-generated hole in the VB). Here, the band structure of the substrate plays a significant role. A change in the surface and bulk electronic structure can dramatically alter the chemical events following photoexcitation of the adsorbate molecules or the catalyst substrate.

2.3. Role of electron scavengers

In the heterogeneous photocatalytic system, electron scavengers play an important role by preventing electron-hole recombination. Oxygen acts efficiently as an electron scavenger, preventing the recombination of photo-generated electrons and holes. When oxygen is limited, the rapid recombination of electrons and holes in TiO_2 would markedly reduce its photocatalytic actions. In lieu of oxygen, inorganic oxidants such as IO_4^-, $S_2O_8^{2-}$, BrO_3^-, ClO_3^-, and H_2O_2 can quench conduction-band electrons and form reactive radical intermediates, thereby reducing the probability of recombination of the photo-generated electrons and holes and enhancing photodegradation of organic substrates by valence holes [45–49]. However, the relative efficiency of these oxidants has not been reported as it varies from system to system.

2.3.1. Oxygen

As described earlier, molecular oxygen (dissolved oxygen in this case) is an efficient electron scavenger and forms O_2^-. Thus, oxygen on the catalyst surface provides a natural sink for the photo-generated electrons. The $O_2^{\cdot -}$ formed in Eq. (6) may generate HP (Eq. (7)) in acidic media [50].

$$O_2^{\cdot -} + e_{CB}^- + 2H^+ \rightarrow H_2O_2 \quad (7)$$

Even though the generation of HP during PCO has been reported long ago, no significant effort has been made to monitor the formation of HP. The HP thus formed may undergo photo-induced degradation, mainly on the photocatalyst surface, by direct reaction with photo-generated charged species, i.e. VB holes, h_{vb}^+, conduction-band electrons, e_{CB}^-, and/or other reactive species such as hydroxyl radicals and the superoxide radical anion. A recent study [51] on photocatalytic degradation of Acid Red 1 (AR1) reported that the highest levels of HP were attained in the presence of P25 (TiO_2). The HP concentration rapidly increased and reached a maximum value corresponding to 80–90% AR1 photodegradation yield and then decreased. An almost identical HP concentration profile was observed during the photocatalytic degradation of benzoic acid in the presence of P25 [52].

2.3.2. Hydrogen peroxide

PCO can be accelerated by HP because it traps e_{CB}^- more efficiently than oxygen. This prevents electron-hole recombination and generates $HO^\cdot$ during the process (Eq. (8)), which has been demonstrated in most studies [53–55]. During the reaction, HP also produces $HO^\cdot$ by reacting with $O_2^{\cdot -}$ or by direct photolysis (Eqs. (9) and (10)). However, when present at high concentration, HP exerts an inhibition effect on PCO by scavenging h_{vb}^+ and $HO^\cdot$ [53,56] (Eqs. (11)–(13)). Furthermore, H_2O_2 can be adsorbed onto TiO_2 particles to modify their surfaces and subsequently decrease their catalytic activity.

$$H_2O_2 + e_{CB}^- \rightarrow HO^\cdot + HO^- \quad (8)$$

$$H_2O_2 + O_2^{\cdot -} \rightarrow HO^\cdot + HO^- + O_2 \quad (9)$$

$$H_2O_2 + h\nu \rightarrow 2HO^\cdot \quad (10)$$

$$H_2O_2 + 2h_{vb}^+ \rightarrow O_2 + 2H^+ \quad (11)$$

$$H_2O_2 + HO^\cdot \rightarrow H_2O + HO_2^\cdot \quad (12)$$

$$HO_2^\cdot + HO^\cdot \rightarrow H_2O + O_2 \quad (13)$$

2.3.3. Peroxydisulphate

The presence of the oxidant peroxydisulphate ($S_2O_8^{2-}$, e.g. $K_2S_2O_8$) also accelerates the PCO process by trapping e_{CB}^- and subsequently preventing its recombination with h_{vb}^+. At the same time, it produces $SO_4^{\cdot -}$, a very strong oxidant ($E^0 = 2.5$–3.1 V vs. NHE) [53] (Eq. (14)). An important advantage of using $S_2O_8^{2-}$ as e_{CB}^- scavenger is that it produces $HO^\cdot$ radicals in aquesous solution at various pH values (Eq. (15)). In fact, $SO_4^{\cdot -}$ starts decomposing into $HO^\cdot$ at $pH > 8.5$, and $HO^\cdot$ becomes the major species at $pH > 10.7$ [57].

$$S_2O_8^{2-} + e_{CB}^- \rightarrow SO_4^{2-} + SO_4^{\cdot -} \quad (14)$$

$$SO_4^{\cdot -} + H_2O \rightarrow SO_4^{2-} + HO^\cdot + H^+ \quad (15)$$

2.3.4. Periodates

Periodate ion has more than two atoms of oxygen per atom of halogen, where I is the central atom. Polarizability differences in the constituent atoms of IO_4^- make its central atom extremely electropositive. Therefore, IO_4^- can capture conduction-band electrons (Eq. (16)) ejected from a photocatalyst more efficiently than other oxidants [45,58–60]. Besides capturing conduction-band electrons, periodate undergoes decomposition under UV-irradiation generating a number of highly reactive radical and nonradical intermediates [61–63] (Eqs. (17) and (18)) including $HO^\cdot$. It has been reported that the reaction rate order with respect to periodate is 0.8 times higher than that for peroxide [58]. The fact that IO_4^- is a more effective oxidant than $S_2O_8^{2-}$ and H_2O_2 for degradation has been reported in some studies [61,62,64]. However, the concentration of IO_4^- in such studies should be optimized, because scavenging of the valuable hydroxyl radicals [65] by IO_4^- ions takes place (Eq. (19)) at higher concentration.

$$IO_4^- + 8e_{CB}^- + 8H^+ \rightarrow 4H_2O + I^- \quad (16)$$

$$IO_4^- + h\nu \rightarrow IO_3^{\cdot -} + O^{\cdot -} \quad (17)$$

$$O^{\cdot -} + H^+ \leftrightarrow HO^{\cdot} \quad (18)$$

$$HO^{\cdot} + IO_4^- \rightarrow HO^- + IO_4^{\cdot} \quad (19)$$

2.3.5. Bromates

Bromate ions as electron scavengers have been rarely studied even though the photocatalytic degradation efficiencies of organic substrates are significantly improved in the presence of $KBrO_3$ [32,54,66]. The enhancement of the degradation is due to the reaction between BrO_3^- ions and conduction-band electrons (Eqs. (20) and (21)), which reduces the electron-hole recombination. It has been shown that BrO_3^- exhibits detrimental effect on the ZnO-catalyzed degradation process at higher concentration due to the adsorption effect of Br^- ion on ZnO surface, which affects the catalytic activity of ZnO.

$$BrO_3^- + 2H^+ + e_{CB}^- \rightarrow BrO_2^{\cdot} + H_2O \quad (20)$$

$$BrO_3^- + 6H^+ + 6e_{CB}^- \rightarrow (BrO_3^-, HOBr) \rightarrow Br^- + 3H_2O \quad (21)$$

2.4. Factors influencing the photocatalytic degradation

2.4.1. Adsorption

It is well established that PCO proceeds through the attack of $HO^{\cdot}$ radicals on the adsorbed surface [67,68]. Thus, the rate of degradation is higher at higher adsorption [69,70]. Adsorption is affected by several factors such as effluent composition and pH. The pH of the reaction medium has a significant effect on the surface properties of TiO_2, which includes the surface charge of the particles, the extent of aggregation of TiO_2 particles and the band edge position of TiO_2. The pH at which the surface of an oxide is uncharged is defined as the zero-point charge (pH_{ZPC}). The pH_{ZPC} of anatase TiO_2, Degussa P-25, Fe_2O_3, CuO, ZnO, ZnS, and CdO are about 4.0, 6.25, 8.6, 9.5, 8.8, 1.7, and 11.6, respectively [21,71–73]. Above and below this value, the catalyst is negatively or positively charged according to Eqs. (22) and (23). Therefore, at $pH < pH_{ZPC}$, the positively charged surface of TiO_2 attracts the anionic species, leading to greater adsorption and hence increased degradation. The reverse effect is observed at $pH > pH_{ZPC}$, where the TiO_2 surface being negatively charged would adsorb cationic species, thereby increasing the degradation efficiency of PCO.

$$Ti - OH + HO^- \rightarrow TiO_2 + H_2O \quad (22)$$

$$Ti - OH + H^+ \rightarrow TiOH_2^+ \quad (23)$$

2.4.2. pH

On the basis of Eq. (4), one can expect that a higher pH value can provide higher concentrations of hydroxyl ions (HO^-) to react with holes to form hydroxyl radicals and subsequent enhancement of PCO. It has been reported that higher pH favors degradation through functional group substitution, while lower pH favors direct ring cleavage prior to the mineralization of organic carbon [74,75]. In addition, it is interesting to note that different proton sources, e.g. HCl, NHO_3, HNO_3, H_2SO_4, H_3PO_4 etc. (i.e. different counter ions associated with protons used for maintaining pH), can alter the photocatalysis to different degrees. It is reported that inorganic anions are capable of inhibiting the photocatalytic degradation of dichloroethane [76] and alachlor, a widely used herbicide [12] in an aqueous suspension of TiO_2. This may be due to the fact that anions may adsorb onto the surface of TiO_2, and isolate the contaminant molecules from the reaction. At pH < pH_{ZPC}, TiO_2 particles are positively charged and the inorganic anions can be attracted towards them forming a layer of charged barriers around TiO_2. This hinders the collision between the target molecule and the TiO_2 particles. Since the density of the hydroxyl radical is highest near the surface of the TiO_2 particles and decreases rapidly with increasing distance from the surface of TiO_2 particles, the inhibition of the coupling of the target molecule with titanium dioxide particles results in rate retardation. This period can be considered as an inhibition period. After this period, the intermediates start accumulating near the TiO_2 particles and may form a bridge or good coupler to couple TiO_2 particles with unreacted contaminant molecules [77]. As the number of the couples increases, they compete with the active sites on the TiO_2 surface with anions and form more couples, thereby progressively reducing the inhibition effect of anions. As a result, the effect of rate of retardation due to the presence of anions is reduced. An interesting result is found with surface-bound phosphate anion [78]. The degradation of substrates (such as 4-chloropehenol, phenol, and rhodamine B) with weak adsorption on the pure TiO_2 was markedly accelerated by phosphate modification, while substrates (such as dichloroacetic acid, alizarin red, and catechol) with strong adsorption exhibited a much lower degradation rate in the phosphate-modified system.

Phosphate anion has a negative effect on the degradation of compounds that can be adsorbed over the catalyst, and a positive effect on the degradation of compounds that hardly adsorb on TiO_2 by enhancing the formation of $HO^\cdot$ radicals in the solution (through the formation of a surface complex), and thus affects the oxidation of those compounds.

2.4.3. Presence of anions

Apart from pollutants, industrial effluents generally contain different salts like chloride, sulphate, bicarbonate, and carbonate. The salts are generally ionized under the conditions accompanying PCO. The presence of an anion or cation affects the rate of PCO. The anions affect the adsorption of the target molecule on TiO_2, act as $HO^\cdot$ scavengers, and may absorb UV light. Negative effects of anions on PCO of aromatic compounds have been reported by some authors [67,79,80]. Recently, the negative effects of Cl^- and NO_3^- ions on the degradation rate of phorate, the restricted pesticides used to control sucking and chewing pests, were reported [81]. It was suggested that the inhibition effect of Cl^- is due to the scavenging of h_{vb}^+ and $HO^\cdot$ (Eqs. (24) and (25)). The radicals ($Cl^\cdot$ and $ClOH^{\cdot-}$) are not as reactive as e_{CB}^- and $HO^\cdot$ and hence cannot contribute towards the degradation process.

$$Cl^- + h_{vb}^+ \rightarrow Cl^\cdot \qquad (24)$$

$$Cl^- + HO^\cdot \rightarrow ClOH^{\cdot-} \qquad (25)$$

The effect of an anion or, in particular, any scavenger of $HO^\cdot$, will depend upon the extent of availability of the scavenger on the surface of the photocatalyst. In other words, conditions which favor adsorption of the scavenger on the photocatalyst will have a negative effect on the rate of PCO. Kamble et al. [82] have shown that HCO_3^- and CO_3^{2-} practically do not adsorb on TiO_2 in the presence of aniline. Further, as the lone pair of electrons in aniline is dispersed over the benzene ring, the site on which aniline is adsorbed develops a negative charge which probably repels HCO_3^- and CO_3^{2-} species. Thus, these species which can scavenge $HO^\cdot$ are effectively eliminated from sites adjacent to those on which aniline is adsorbed. These sites then become available for the generation of $HO^\cdot$. These factors contribute to the enhanced PCO of aniline in the presence of HCO_3^- and CO_3^{2-}.

2.4.4. Presence of cations

The presence of transition metal ions was found to increase the TiO_2 photocatalytic degradation of organic pollutants [83–88]. The observed rate increase has been attributed to the tendency of the metal ions to be reduced at the semiconductor surface by scavenging e_{CB}^- (Eq. (26)).

$$M^{n+} + e_{CB}^- \rightarrow M^{(n-1)+} \qquad (26)$$

where M^{n+} represents the most extensively studied metal ions to enhance the photocatalytic degradation rates, viz. Fe^{3+}, Mn^{3+}, and Cu^{2+}. The above reaction prevents electron-hole recombination and results in an increased rate of formation of $HO^\cdot$ radicals. Transition metal ions also increase PCO rate by inducing photo-Fenton type reactions (Eq. (27)) to produce more $HO^\cdot$ radicals [85].

$$M^{(n-1+)} + H_2O_2 + H^+ \rightarrow M^{n+} + HO^\cdot + H_2O \qquad (27)$$

The effect of Fe^{3+} ions on the photodegradation of OCs has been investigated extensively. It is found that ferric ions increase the degradation rate up to a certain concentration, beyond which the rate begins to decrease [83–85,87]. Butler et al. [87] have also reported the positive effect of Mn^{2+} ions on the photocatalytic degradation of organic pollutants. However, there is considerable controversy on the photocatalytic activity of cupric ions. Some investigators [86–88] have found that cupric ion behaves as an accelerator, where as some others [83,84] have reported a decrease in the apparent rate constant upon the addition of cupric ions. The negative effect of cupric ions on the photocatalytic degradation may be attributed to the low reduction potential for Cu^{2+}/Cu^+ couple. As a result, cupric ions are reduced to cuprous by e_{CB}^- (Eq. (28)). The Cu^+ ions thus formed are oxidized to Cu^{2+} ions either by h_{vb}^+ on the surface of the TiO_2 particles or by $HO^\cdot$ radicals (Eqs. (29) and (30)). This causes a decrease in the concentration of $HO^\cdot$ and hence a decrease in the degradation rate.

$$Cu^{2+} + e_{CB}^- \rightarrow Cu^+ \qquad (28)$$

$$Cu^+ + h_{vb}^+ \rightarrow Cu^{2+} \qquad (29)$$

$$Cu^+ + HO^\cdot + H^+ \rightarrow Cu^{2+} + H_2O \qquad (30)$$

2.4.5. Temperature

An increase in reaction temperature generally results in increased photocatalytic activity. However, reaction temperature greater than 80˚C promotes the recombination of charge carriers and disfavors the adsorption of OCs on the TiO_2 surface. Normally, a photocatalytic reaction has an optimum range of operational temperature between 20 and 80˚C as mentioned by Hermann [3] as well as Gogate and Pandit [2]. When working at a low temperature, desorption of the products formed limits the degradation reaction. On the other hand, at a higher temperature, adsorption of the OC on the TiO_2 surface becomes the limiting stage. The optimum range of temperature has a small effect on reaction rate, as long as the experiment is carried out near the middle of the range of 20–80˚C. When the optimum range of temperature is from 40 to 50˚C, the increase from 40 to 50˚C does not affect the reaction rate [89]. A reaction temperature below 80˚C favors the adsorption whereas further reduction of reaction temperature to 0˚C results in an increase in the apparent activation energy. Therefore, temperature range between 20 and 80˚C is regarded as the desired temperature for effective photomineralization of OCs.

Photocatalytic reactions at the temperature of 38–100˚C seem to followed pseudo-first-order rate law, and the temperature affects the reaction rate highly. The rate constants increase by about six times from 3.52×10^{-4} to $2.17 \times 10^{-3}\,\text{min}^{-1}$ when the temperature is adjusted from 38 to 100˚C. Consequently, this photocatalytic course can be accelerated by using the infrared light of solar energy to increase the temperature of the photocatalytic reaction. It should be a potential way to make full use of solar light in photocatalysis in practice [90].

3. Kinetics of photocatalytic degradation

Langmuir–Hinshelwood model as defined by Eq. (31) has been widely applied for the analysis of heterogeneous photocatalytic degradation kinetics of pollutant OC in the aqueous phase [91]:

$$r_0 = -\mathrm{d}C/\mathrm{d}t = -k\mathrm{KC}/(1+\mathrm{KC}) \tag{31}$$

where r_0 is the initial reaction rate (mg $\text{l}^{-1}\,\text{min}^{-1}$), C is the concentration of OC ($\text{mg}\,\text{l}^{-1}$), t is the reaction time (min), k is the Langmuir–Hinshelwood reaction rate constant ($\text{mg}\,\text{l}^{-1}\,\text{min}^{-1}$), and K is the Langmuir adsorption equilibrium constant ($\text{l}\,\text{mg}^{-1}$). At a dilute concentration of OC (i.e. KC<<1) [10], pseudo-first-order kinetic model can be assumed (Eqs. (32) and (33)),

$$r_0 = -\mathrm{d}C/\mathrm{d}t = k\mathrm{KC} \tag{32}$$

$$\ln(C/C_0) = -k\mathrm{Kt} = -\mathrm{K}_{\mathrm{app}}t \tag{33}$$

where K_{app} (min^{-1}) is the apparent rate constant, and C_0 is the initial concentration of OC (mg l^{-1}).

In addition to the Langmuir–Hinshelwood model and pseudo-first-order kinetic model [92,93], a pseudo-second-order kinetic model (Eq. (34)) has been used to describe the degradation kinetics of different compounds [94].

$$-\mathrm{d}C/\mathrm{d}t = kC^2 \tag{34}$$

where k ($\text{mg}^{-1}\ \text{l}\,\text{min}^{-1}$) is the second-order kinetic constant.

It is found that the degradation rate depends on the initial concentration of the OC. The kinetics of photocatalytic degradation of OC is shown in Fig. 2 plotting concentration against time. Since hydroxyl radicals have a very short lifetime (only a few nanoseconds), they can react only at or near the location where they are formed. A high OC concentration increases the probability of collision between an organic matter and an oxidizing species, leading to an increase in the mineralization rate. The values of ln (C_0/C) vs. time are plotted in Fig. 2 (in set). The figure shows that the photocatalytic degradation follows the pseudo-first-order kinetics with respect to OC concentration.

The effect of initial OC concentrations on the initial rate of degradation is shown in Fig. 3. A linear expression can be obtained conventionally by plotting the reciprocal apparent rate constant against the initial concentration (plot of $1/K_{\mathrm{app}}$ against C_0) as

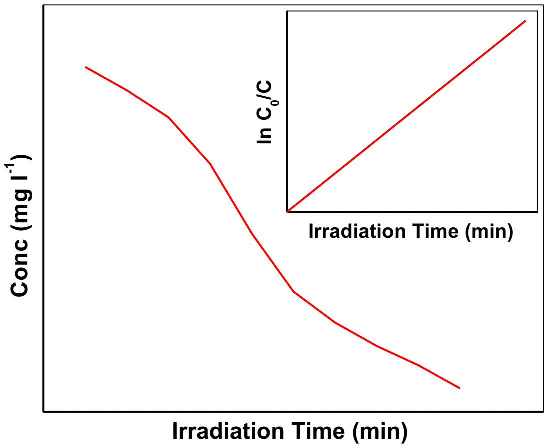

Fig. 2. Kinetics of photocatalytic degradation at initial concentration. Inset: first-order plot for photocatalytic degradation of organic compound.

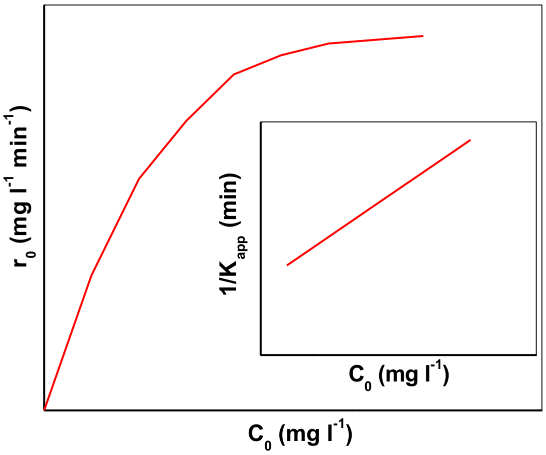

Fig. 3. Effect of initial concentration on the initial rate of degradation. Inset: reciprocal of apparent rate of degradation against initial concentration.

shown in Fig. 3 (inset). In general, experimental data fit well to the second-order kinetic model for the early minutes of irradiation when the OC concentration is high [95]. A possible explanation for second-order photodegradation kinetics is the aggregation or dimer formation with increasing OC concentration [96]. Experiments carried out with low concentrations are usually described by the pseudo-first-order kinetic model [94]. In general, the value of the second-order kinetic constant was lower when the amount of OC was increased for the same amount of catalyst [95].

4. Modified photocatalysis

4.1. Modification technology

In heterogeneous photocatalysis, the limitation of the photocatalytic degradation is attributed to the recombination of photo-generated electron-hole pairs. As discussed earlier, various attempts have been made to avoid this recombination in photocatalytic processes. Another limitation of this process is that TiO_2 can absorb UV light effectively but not visible light. More recently, significant efforts have been made to develop new techniques or modified semiconductor photocatalysts that are capable of absorbing visible light (400–700 nm). These include metallic and nonmetallic element doping, sensitization with organic dyes, and development of small band-gap semiconductors. Besides, noble metal ion implantation and nano semiconductor composite catalysts are developed as other alternatives. The structural modification is also extended to separate and recover titania after the process of photocatalysis [97].

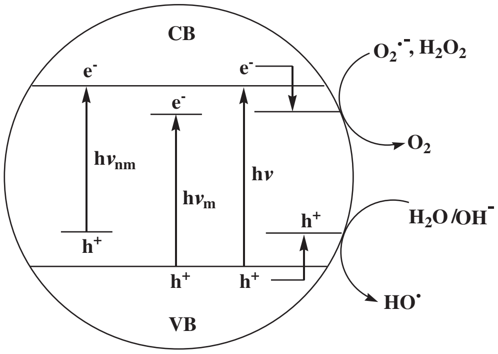

Fig. 4. Simplified mechanism of pure and doped TiO_2 photocatalysis: doping reduces band gap facilitating photoexcitation and production of reactive radicals. hυ—pure TiO_2; hν_m—metal-doped TiO_2; hν_m—nonmetal-doped TiO_2.

4.2. Doping

Doping of ions or atoms causes the TiO_2 lattice to modify its micro and electronic structures, and the introduced defects distort TiO_2 lattice and inhibit anatage to rutile transformation. Moreover, alternative energy levels in between bands and so mid-gap energy levels below conduction band or above VB are formed (Fig. 4). Both metal and nonmetal atom impurities serve as trapping centers to retard charge recombination and extend the excitation wave length from the UV to the visible-light range.

4.2.1. Metal ion doping

The doping of metal ions into the TiO_2 lattice works wonderful as the resulting materials show an enhancement of photocatalytic properties. In recent years, extensive research focuses on visible-light-induced metal ion-doped semiconductor photocatalysis. Studies show that the role of metal ion doping to enhance photocatalytic activities is mainly due to the following modification mechanisms:

(1) reduction of the band gap in titania, [98]
(2) improvement in charge carrier separation, [99] and
(3) increase in the level of surface-adsorbed species, e.g. hydroxyl radicals [100].

The visible-light photoactivity of metal-doped TiO_2 can be explained by a new energy level produced in the band gap of TiO_2 by the dispersion of metal nanoparicles in the TiO_2 matrix. As shown in Fig. 4, electron can be excited from the defect state to the TiO_2 conduction band by photon with energy equals to hν_m. The additional benefit of metal ion doping is the trapping of electrons to restrain electron-hole recombination and leave the holes for oxidative degradation of OCs. Further, metal ion doping enhances interfacial charge transfer reactions, thereby increasing the photoreactivity of TiO_2 [101]. The doping of metal ion induces a red shift of absorption capacity from UV to visible region by introducing a localized band of orbital within the band gap. Recently, most of the investigations have focused on preparing TiO_2 catalysts which can be activated by visible light because there is much more energy produced by the sunlight in the visible-light region compared to the UV region [18,102,103]. As mentioned, doping or combining of TiO_2 with various metal ions was reported as a good tool to improve the photocatalytic properties [104] and for enhancement of visible-light response [105,106]. Numerous metal ions, including transition metal ions (e.g. vanadium, chromium, iron, nickel, cobalt, ruthenium and platinum) and rare earth metal ions (e.g. lanthanum, cerium, and ytterbium), have been investigated as potential dopants for visible-light-induced photocatalysis. However, as will be discussed later, metal ion dopant can also serve as a recombination center, resulting in decreased photocatalytic activities.

4.2.2. Transition metal ion doping

The sol–gel method has been widely used to prepare titania nanoparticles under controlled conditions [107]. The integration of dopants into the sol during the gelation process facilitates direct interaction with TiO_2. Therefore, dopants can be incorporated into the titania lattice, resulting in materials with different optical and catalytic properties. Paola et al. [101] used a set of TiO_2 photocatalysts loaded with various transition metal ions (Co^{2+}, Cr^{3+}, Cu^{2+}, Fe^{3+}, Mo^{5+}, V^{5+}, and W^{6+}) and tried to find a correlation between photocatalytic behavior and physicochemical properties of prepared samples. They have reported a descending sequence of photocatalysts depending on their activities: $W/TiO_2 > Mo/TiO_2 > Cu/TiO_2 > Fe/TiO_2 > Co/TiO_2 > V/TiO_2 > Cr/TiO_2$. Chen and Wang [108] have demonstrated that different metal ion doping exhibits complex effects on the characteristics of titania. Across the investigated ions ($Zn^{2+}, Fe^{3+}, Co^{2+}, Cu^{2+}, Ni^{2+}, Mn^{2+}, V^{5+}, Cr^{3+}$), doped TiO_2 has shown the higher photoactivity in the decoloration of methyl orange compared with bare TiO_2. Sharma et al. [109] found increased catalytic activity of titania films on methyl orange degradation when doped with 2–10 mol% Ni. Wu and Chen [110] directed their research at developing a visible-light response catalyst via vanadium doping and evaluated the higher activity of V/TiO_2 on the degradation of crystal violet and methylene blue under visible-light irradiation. They found that an increase in vanadium doping promoted particle growth, in which vanadium, as per X-ray absorption spectroscopy (XAS) analysis, is highly dispersed inside the titania structure. This results in enhanced "red-shift" in the UV–vis absorption spectra and subsequent higher activity of TiO_2.

Indeed, special efforts have been dedicated to doping TiO_2 with Fe^{3+} ions [111–113]. Amongst a variety of transitional metals, iron is suitable for doping because of the fact that the radius of Fe^{3+} (0.79 Å) is similar to that of Ti^{4+} (0.75 Å), so that Fe^{3+} can be easily incorporated into the crystal lattice of TiO_2. This interest is based on the idea that Fe^{3+} ions act as shallow charge traps in the TiO_2 lattice [99,114,115]. However, the role of Fe^{3+} ions in TiO_2 is controversial. Some authors suggest that Fe^{3+} behaves as e^-, h^+ recombination center [116], while others have postulated that the role of dopant ion is to favor e^-/h^+ separation, which enhances the photoactivity [70,99,111,112]. Nano-sized Fe-doped and undoped TiO_2 particles have been synthesized by hydrothermal process at low temperature [117]. Doping of TiO_2 by Fe^{3+} ion decreases the particle size resulting in an increase in the surface area. They have demonstrated higher photocatalytic performance of Fe-doped TiO_2 thin film than that of the undoped TiO_2 film under UV and visible lights for the degradation of Malachite green. They have also suggested that the interaction of Malachite green with Fe^{3+}-doped TiO_2 thin films follows the pseudo-first-order reaction kinetics. Nano-sized titania homogeneously doped with chromium has also been prepared through the sol–gel method [107]. Substantial doping can be achieved until 1.0 wt. % of chromium content is reached. Chromium in titania-doped materials can have other oxidation states than that exhibited in its precursor because of the possibility of redox reactions during the synthesis. The visible-light absorption by chromium-doped TiO_2 is believed to be due to a different mechanism, i.e. chromium doping does not bring down the band gap, but induced visible-light absorption through the formation of color centers.

4.2.3. Noble metal atom doping

Given that charge separation enhances photocatalytic activity, one clever way of achieving charge separation, as well as visible-light activity, is to incorporate noble metal nanoparticles such as silver or gold into the titanium dioxide material. For example, incorporation of a small amount of silver (1–5%) results in increased efficiency in photocatalysis [118]. Silver has a "Fermi level" or electron-accepting region at an energy level just below its conduction band. Therefore, after light absorption and charge separation, the electron in the conduction band can be effectively trapped by silver, while the hole oxidizes water and forms hydroxyl radicals, without the threat of recombination. Thus, silver nano-particles facilitate longer charge separation by trapping photo-generated electrons as shown in Fig. 5. Various researchers have shown that there is an optimum amount of silver to be added—just enough is needed so that silver sites are dispersed through the material to rapidly trap electrons. On the other hand excess of silver may cover the titanium dioxide and prevent light absorption. In addition, too much silver may mean that the silver acts as a recombination site itself—essentially, it will form a bridge between an electron and a hole [119]. The emission of titanium dioxide (and of similar studies with zinc oxide) can be interpreted as a measure of the recombination efficiency. Studies examining the emission of these metal oxides have demonstrated that the emission intensity reduces on increasing the load of silver—indicating that the silver traps electrons and reduces electron-hole recombination. The higher efficiency of Ag^+-doped TiO_2 has been reported in the photocatalytic degradation studies of C.I. basic violet 3 [120] and Acid Red 88 [118]. Ag–AgCl-modified TiO_2 has been used for the degradation of 4-Chloro phenol [121] working under visible radiation. Studies have revealed that the photocatalytic activity of TiO_2 can be improved significantly by doping with noble metals such as Pt, Au, and Ag [122–127]. Under UV irradiation, the photo-generated electrons quickly transfer from TiO_2 surfaces to the Pt particles, leading to an effective separation of electron hole and resulting in the improvement of photocatalytic efficiency. Preparation of Pt-modified TiO_2 loaded on natural zeolites (Pt–TiO_2/zeolites) by sol–gel technique photoreductive deposition method was reported by Huang et al. [128]. Their photocatalytic activities were examined by photocatalytic decolorization of methyl orange solution under UV-light irradiation. The results show that Pt doping induces enhancement of photocatalytic decolorization.

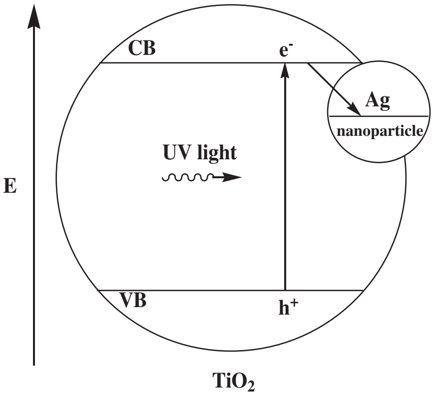

Fig. 5. Simplified mechanism of photoexcitation of heterostructure formed by incorporation of silver nanoparticles to TiO_2 that facilitates longer charge separation by trapping photogenerated electrons.

4.2.4. Nonmetal atom doping

There are three main opinions regarding nonmetal doping as modification mechanism:

(1) Band gap narrowing [129];
(2) Impurity energy level [130]; and
(3) Oxygen vacancies [131].

It is found that cationic or metal dopants usually induce localized dopant levels deep in the band gap of TiO_2, which often serve as recombination centers for photo-generated charge carriers [132]. Thus nonmetal dopants, such as carbon (C), nitrogen (N), and sulphur (S), may be more appropriate for an extension of photocatalytic activity into the visible-light region because the related impurity states are supposed to be close to the VB maximum. The studies of visible-light active semiconductors doped with nonmetallic elements such as N, S, and C have been extensively carried out since the first-ever study of N-doped TiO_2 by Asahi and co-workers was published in 2001 [129]. Matsumoto et al. [133] prepared an N-doped titania from a layered titania/isostearate nanocomposite. N-doping can be achieved by various methods such as sputtering TiO_2 targets in N_2–Ar atmosphere [129]; treating of TiO_2 powders in an ammonia atmosphere over several hundred centigrades [130]; heating TiO_2 powders with urea [134]; and hydrolyzing organic or inorganic titanium compounds such as titanium tetraisopropoxide or titanium tetrachloride in ammonia solution, by direct amination of TiO_2 nanoparticles with triethylamine [135]. The investigation of the efficiency of N-doped TiO_2 as a photocatalyst in the degradation of the herbicide mecoprop ($C_{10}H_{11}ClO_3$) was studied by Abramović et al. [136] and it was found that the efficiency of N-doped TiO_2 was 1.5 times more than that of Degussa P-25. Recently, Nitrogen-doped TiO_2 prepared by sol–gel method [137] has been used to study the effect of temperature on the nature of band gap to create a visible-light active photocatalyst. N-doped TiO_2 is by far the most intensively studied system followed by carbon-doped titanium dioxide in harvesting solar light for photocatalytic activity [138]. Yang et al. [139] synthesized a carbon-doped TiO_2 and both carbon- and vanadium-doped TiO_2 by the sol–gel process. Both the catalysts show higher activity under visible light for acetaldehyde degradation. Moreover, the doped carbon increased the surface area and improved the dispersion of vanadium. Recently, it has been reported that carbon doping has the best photoresponse compared to other nonmetals. Also, carbon present in titanium dioxide particles is assumed to play as a sensitizer in photocatalytic reaction [140]. Lettmann et al. [141] have obtained photo-stable carbon-modified TiO_2 photocatalyst by the pyrolysis of titania alcoholic suspension and proved that the increase of photocatalytic activity of new material under visible-light irradiation was due to the effect of carbon presence in TiO_2 lattice. Matos et al. [142] and Janus et al. [143] also reported the higher photocatalytic activity of C-doped TiO_2 during the methylene blue decomposition under visible light. Ohno et al. [132] have synthesized chemically modified titanium dioxide photocatalysts in which S substitutes for some of the lattice titanium atoms. They show strong absorption for visible light and high activities for degradation of methylene blue, 2-propanol in aqueous solution, and partial oxidation of adamantane under irradiation longer than 440 nm. Visible-light-induced degradation of phenol using S-doped TiO_2 has also been successfully reported by Rockafellow et al. [144]. Recently, Se(IV)-doped TiO_2 reported by Yelda et al. [145] shows the enhanced degradation rate of 4-nitro phenol under both UV-A and sunlight irradiation.

There has been some discussion in the literature on the mechanism of the enhancement of photocatalytic activity by nitrogen doping. It was originally proposed that N doping of TiO_2 can shift its photoresponse into the visible region by mixing of p states of nitrogen with 2p states of lattice oxygen and by increasing the photocatalytic activity by narrowing the TiO_2 band-gap [129]. However, more recent theoretical and experimental studies have shown that the nitrogen species result in localized N-2p states above the VB and the electronic transitions from localized N-2p state to the CB are made in TiO_2 under visible-light irradiation [97,130,146–150]. The other mechanism put forward by Nakamura et al. [151] and Irie et al. [130] counters Asahi's original explanation that the N-doping reduces the gap between the VB and conduction band of titania. These researchers propose that N-doping introduced new occupied (i.e. electron rich) orbitals in between the VB (which are comprised primarily of O-2p orbitals) and the conduction band (which are comprised primarily of Ti-3d orbitals). These N-2p orbitals act as a step-up for the electrons in the O-2p orbital. Electrons from N-2p orbitals need much smaller jump to be promoted into the conduction band. Once this process occurs, electron from the original VB can migrate into the mid band-gap energy level, leaving a hole in the VB. Thus, N-doping results in a mid-band-gap energy level which reduces the energy gap and thus utilizes visible light instead of UV light for photoexcitation as shown in (Fig. 6). Unlike metal ion doping, nonmetallic dopants replace lattice oxygen and are less likely form recombination centers.

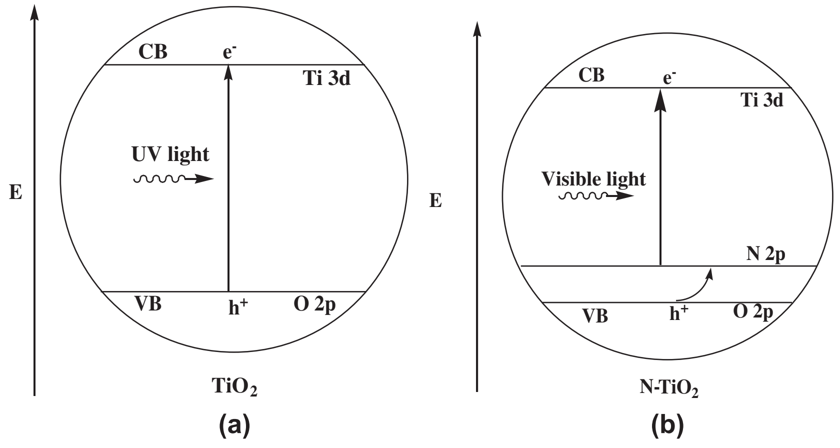

Fig. 6. (a) Simplified mechanism of photocatalysis with undoped TiO_2; it requires UV light due to large band gap. (b) Simplified mechanism of N-doped TiO_2 showing step-by-step photoexcitation in which N-2p orbitals act as a step-up for the electrons in the O-2p orbitals that results in a mid band-gap energy level which reduces the band gap and utilizes visible light.

4.3. Heterojunction composite photocatalyst

Synthesis of composite photocatalyst leads to the visible-light-sensitive photocatalysis having higher photocatalytic activity than pure TiO_2. In composite semiconductor photocatalyst, the CB electrons photogenerated from a small band-gap semiconductor by the absorption of visible light can be injected to the CB of a large band-gap semiconductor, while the photo-generated holes are trapped in the small band-gap semiconductor (Fig. 7). Thus, an effective electron-hole separation can be achieved. A similar strategy to that described above, in a rapidly evolving area, is the idea of incorporating different semiconductors which have different conduction-band energy levels. The strategy is as before, to trap the electron so that the hole can have more time to react. A simple example is the anatase–rutile heterojunction. Rutile has a smaller band gap (by about 0.2 eV) than anatase, although its VB levels are at similar energies. Therefore, in an analogous fashion to the situation with silver (Fig. 5) as described earlier, charge separation in anatase, followed by electron injection into the less positive rutile conduction band [152] means that there is a hole in the VB of anatase that can freely oxidize water. This also reduces the rate of recombination of electrons and positive holes in the anatase part.

A nanocrystal heterojunction of $LaVO_4/TiO_2$ visible-light photocatalyst has been successfully prepared using a simple coupled method by Huang et al. [153]. The results show that such nanocomposite catalysts exhibit strong photocatalytic activity for decomposition of benzene under visible-light irradiation with high photochemical stability. The enhanced photocatalytic performance of $LaVO_4/TiO_2$ may be attributed to not only the matched band potentials but also the interconnected heterojunction of $LaVO_4$ and TiO_2 nanoparticles. The development of heterojunction semiconductor extends the photosensitivity of TiO_2 into the visible region [154,155]. This technique has advantage over metal- and anion-doped TiO_2 catalyst in that the latter becomes impaired by an increase in carrier-recombination facilities or thermal instability because of photocorrosion or rapid recombination of photo-generated electron-hole pairs. It is assumed that $LaVO_4$ may function as a sensitizer to absorb visible light and the heterojunction of $LaVO_4/TiO_2$ may act as an active center for hindering the rapid recombination of photo-induced electron-hole pairs generated by $LaVO_4$. When visible light is supplied to the $LaVO_4/TiO_2$ heterojunction, electrons and holes generated by $LaVO_4$ are separated. Some electrons are injected into TiO_2 nanoparticles quickly since the conduction band of $LaVO_4$ is more negative than that of TiO_2. Moreover, the nanostructure heterojunction on $LaVO_4/TiO_2$ composite also leads to a more efficient inter electron transfer between the two components. Furthermore, the large specific surface area of $LaVO_4/TiO_2$ nanocomposite was also favorable for photocatalytic reaction. The photocatalytic activity of SiO_2–TiO_2 composite photocatalyst prepared by sol–gel method with the assistance of sodium dodecyl benzene sulphonate is found to be very high during the decolorization of methyl orange solution [156]. To sum up, the improvement of charge separation, efficient inter electron transfer, the generation of $HO^•$, and large specific surface area were supposed to be responsible for the high efficient photocatalytic activity of the $LaVO_4/TiO_2$ nanocomposite as well as SiO_2–TiO_2 composite. The photocatalytic activity of a mesoporous TiO_2-pillared hexaniobate nanocomposite has been successfully studied in the degradation of acid red G [157].

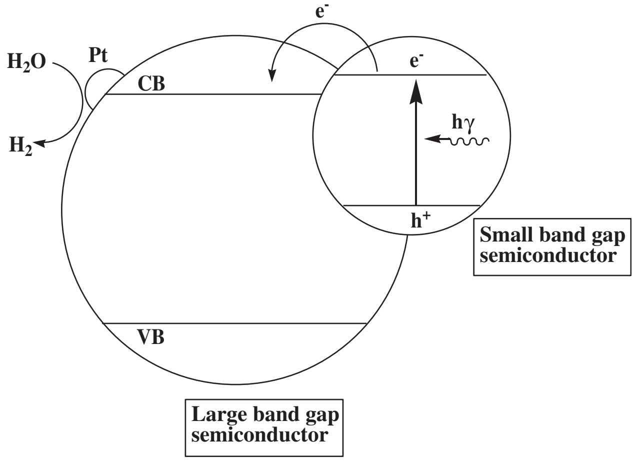

Fig. 7. Simplified mechanism showing interparticle electron transfer process from CB of photo-excited small band-gap semiconductor to CB of TiO_2 in composite photocatalyst.

4.4. Dye sensitization

A better method to achieve the utilization of visible light for TiO_2 is dye sensitization. It is most popular and successful for solar-cell applications [158,159] and hydrogen production. It is found that metal dopants induce localized d-levels deep in the band gap of TiO_2, which often serve as recombination centers for photo-generated charge carrier. The doping process of the nonmetal elements always involves thermal treatment at high temperatures [130,151] or a long time of hydrothermal treatment [160], both of which are energetically unfavorable. Visible-light-induced dye-sensitized TiO_2 photocatalysts are readily prepared under a mild condition through interfacial adsorption of dye molecules on TiO_2 in an ambient environment [161,162].

A visible-light TiO_2 photocatalyst was prepared by a surface chemical modification process with toluene 2,4-diisocyanate (TDI) [163]. The TiO_2–TDI photocatalyst has an obvious absorption in visible region, which is proposed as the direct surface electron transfer from the lone pair electrons of N atom (597 nm) and O atom (469 nm) to the conduction band of TiO_2. TiO_2–TDI photocatalyst exhibits a satisfactory photostability and high photocatalytic performance for the degradation of phenol, 2, 4-dichlorophenol, fluorescein, and methyl orange [162]. Results also show an enhanced photo catalytic efficiency of decomposing methylene blue in the presence of dye-sensitized $(TiO_2)_8SBA$ under visible-light and solar-light irradiation [164]. In another study, dye-sensitized TiO_2 nanoparticles loaded with $Al_2O_3/TiO_2/Pt$ were synthesized and investigated to show enhanced activity under visible light for the production of hydrogen [165]. The different steps of electron transfer/recombination processes occurring on a dye-sensitized TiO_2 particle are:

- Dye excitation;
- Electron injection /transfer from excited dye to TiO_2 CB;
- Electron trapping on substrate; and
- Back electron transfer to oxidized dye (recombination).

where D stands for sensitizer, D^* for the electronically excited sensitizer, and D^{*+} for the oxidised sensitizer. The vis-TiO_2 photocatalysis involves the following sequence of reactions:

$$D + h\nu \text{ (visible)} \rightarrow D^* \tag{35}$$

$$D^* + TiO_2 \rightarrow D^{*+} + e^-_{TiO_2} \tag{36}$$

$$e^-_{TiO_2} + O_2 \rightarrow TiO_2 + O_2^{\cdot -} \tag{37}$$

$$D^{*+} + e^- \rightarrow D \tag{38}$$

Dye-sensitized photocatalysis begins with the visible-light absorption of dye and a subsequent electron transfer from the excited dye to the conduction band of TiO_2 as shown in Fig. 8. However, the electron transfer from excited dye to TiO_2 usually depends strongly on the adsorption efficiency of dye molecules and it can be deeply depressed by the competitive adsorption of other co-existing species in the solution. Considering that pollutants usually exist at high concentration in the practical wastewaters, dye-sensitized photocatalysis may face difficulties of keeping valuable electron transfer efficiency. The mechanism is based on the absorption of visible light for exciting an electron from the highest occupied molecular orbital to the lowest unoccupied molecular orbital of a dye. The excited dye molecule subsequently transfers electrons into the conduction band of TiO_2, and is converted to its cationic radical. The TiO_2 acts only as a mediator for transferring electrons from the sensitizer dye to the substrate on the TiO_2 surface and the VB of TiO_2 remains unaffected. The injected electrons jump to the surface of titania where they are scavenged by molecular oxygen to form superoxide radical, $O_2^{\cdot -}$ (Eq. (37)) and hydrogen peroxide radical, $^{\cdot}OOH$. These reactive species, on disproportionation, produce hydroxyl radicals. The subsequent reactions lead to the degradation of the pollutant.

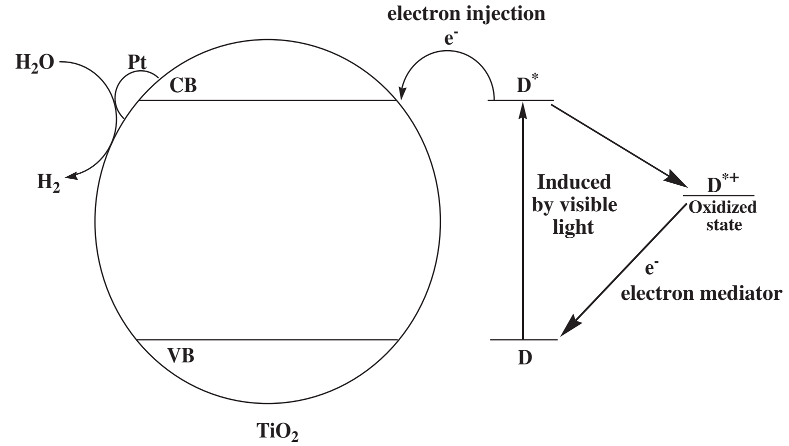

Fig. 8. Simplified mechanism of visible-light-induced dye-sensitized photocatalysis showing electron transfer from the excited dye to CB of TiO_2.

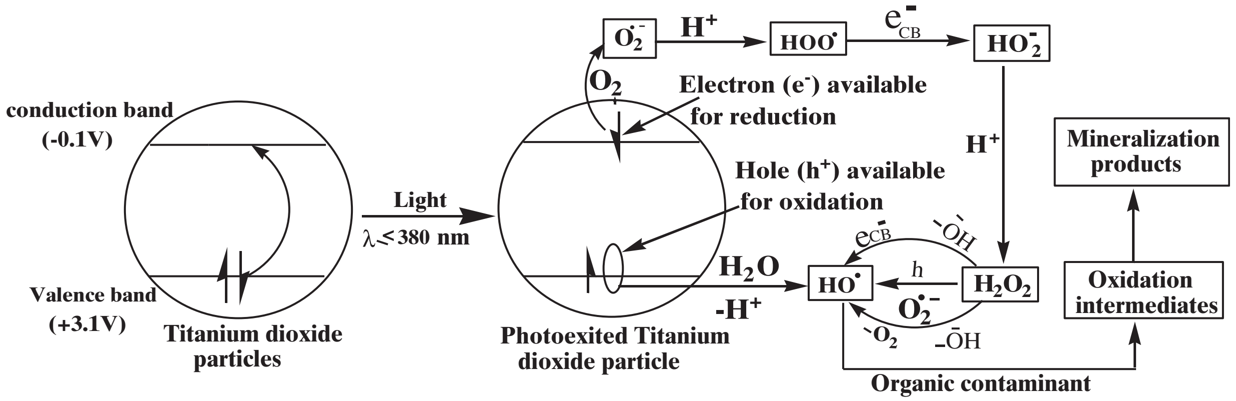

Fig. 9. Simplified diagram showing TiO_2 photocatalytic mineralization of organic contaminants. Hydroxyl radicals oxidize organic contaminants to intermediates leading to mineralization products.

5. Applications of photocatalysis

5.1. Environmental remediation

The field of heterogeneous photocatalysis has expanded rapidly, undergoing various evolutionary phases related to environment and energy. Titanium dioxide offers a great potential as a catalyst material for its use in industrial technology in the environmental remediation. Its capacity in oxidizing substances arises from the generation of highly reactive oxygen species (ROS) such as OH and superoxide radicals on the surface of TiO_2. The organic pollutants present in water subsequently react with ROS, holes, or electrons, and they undergo a series of redox chemical reactions, eventually leading to mineralization. The sequence of events leading to the mineralization of OCs using TiO_2 as a photocatalyst is presented in Fig. 9. In this process, the pollutants are degraded by UV irradiation ($\lambda \leqslant 380\,\text{nm}$) of a semiconductor suspension of titanium dioxide based on the formation of ROS. The preferred oxidation route is highly target molecule-dependent. Those species that adsorb strongly to TiO_2 (highly polar compounds) are more likely to oxidize via the photo-generated holes.

Photo-induced redox reactions on TiO_2 can also transform a variety of inorganic pollutants such as oxyanions (arsenates, chromate, bromated, etc.), ammonia, and metal ions. The photo-induced ROS generation on C is exploitable for bacterial/viral inactivation as well. Photocatalysis is therefore, a potential tool for the treatment of different types of aquatic pollutants to get remediated. Many of the air pollutants are also got remediated, exploiting photo-induced redox reactions. The development in the field of TiO_2 photocatalsis has been utilized for a wide range of environmental and energy applications [166].

5.1.1. Water treatment

Treatment of water can be accomplished by adding a powdered form of TiO_2 in the water, or it can be immobilized on a substrate. If TiO_2 is in solution then some sort of recovery system is necessary in order to reuse the catalyst. Photocatalysis has been proven to remove not only both organic and inorganic pollutants in addition to trace metals from water, but also nuisance color, taste, and odor compounds. Conventional as well as modified TiO_2 has been extensively studied for water treatment and it is well known to be an effective system to treat several hazardous compounds in contaminated water.

Photocatalysis has been used for the destruction of OCs such as alcohols, carboxylic acids, phenolic derivatives, or chlorinated aromatics, into harmless products as carbon dioxide, water, and simple mineral acids [67,167,168]. In addition to OCs, wide ranges of inorganic compounds are sensitive to photochemical transformation on the catalyst surfaces. Inorganic species such as bromate, or chlorate, azide, halide ions, nitrate ions, nitric oxide, palladium, and rhodium species, and sulfur species can also be decomposed [169,170] by photocatalysis. Metal salts such as $AgNO_3$, HgCl, and organometallic compounds (e.g. CH_3HgCl) as well as cyanide, thiocyanate, ammonia, nitrates and nitrites can be removed from water [67,171].

Trace metals, such as mercury (Hg), chromium (Cr), lead (Pb), cadmium (Cd), arsenic (As), and others metals are considered to be highly health hazardous. Thus, the removal of these toxic metals is essentially important for human health and water quality [67,172]. The environmental applications of heterogeneous photocatalysis include the removal of heavy metals such as (Hg), chromium (Cr), lead (Pb), Cadmium (Cd), lead (Pb), Arsenic (As), nickel (Ni), and cupper (Cu) [171]. It is seen that modified photocatalyst TiO_2/Al_2O_3 is efficient in the removal of toxic pollutant like surfactant Triton X-100 from model wastewater [173].

Matsunaga et al. [174] were the first to demonstrate the photochemical sterilization method. Microbial cells were killed photochemically with semiconductor power of titanium dioxide deposited on platinum (TiO_2/Pt). The cell was photo-electrochemically oxidized; as a result, the respiration of cell was inhibited leading to its death. Bacteria and viruses like *Streptococcus Streptococcus natuss, Streptococcus cricetus, Escheria coli (E. coli), Scaccharomyces cerevisisas, Lactobacillus acidophilus, and Poliovirus I* have been destructed effectively using heterogeneous photocatalysis [175–177]. Photo-disinfection sensitized by TiO_2 has some effect on the degradation of *Chlorella vulgaris* (Green algae), which has a thick cell wall. It is reported that photocatalysis removes not only pollutants from water but also color, taste, and odor from water. With respect to the algal bloom in fresh water supplies and the consequent possibility of cyanobacterial microcystin contamination of potable water, microcystin toxins, present in algal water, are reported to be degraded on immobilized TiO_2 catalyst [178]. An analysis by electrophoresis has revealed that bacterial DNA and RNA molecules completely disappear after 7 h of photocatalytic treatment. The antibacterial activity of TiO_2 is related to ROS production, especially hydroxyl free radicals and peroxide formed under and reductive pathways, respectively. Some reviews on photocatalytic disinfection and its mechanism have also been published recently [179–181]. The nano-sized TiO_2 was also reported to kill viruses including polio virus 1, hepatitis B virus, herpes simplex virus, and MS2 bacteriophage [182].

An attractive feature of TiO_2 photocatalytic disinfection is its potential to be activated by visible light. It has been demonstrated that doping TiO_2 with silver has greatly improved photocatalytic inactivation of bacteria [183] and viruses [184]. Recently, the antimicrobial activity of silver-deposited TiO_2 nanocomposites, $Ag^+/TiO_2–TiO_2O_3$, has shown to exhibit a good bactericidal activity against *E. coli* under visible light [185] and the role of ROS in the photocatalytic bacterial disinfection process in presence of a visible-light-active photocatalyst, B-N-co-doped TiO_2 has been investigated [186].

5.1.2. Air treatment

Air contains avariety of volatile organic compounds (VOCs) which are hazardous to health. These VOCs are emitted into the atmosphere by a wide variety of industrial processes and cause adverse effects on human nervous system, via breathing. The indoor air shows high level of pollutants than that of the nearby outdoor air. Indoor air refers to air of any confined place having levels of pollutant which are above the ambient concentrations outside of the confined place. Among the air contaminants, one finds formaldehyde, acetaldehyde, aromatic hydrocarbons, NO_x, and CO. Photocatalysis well suits for the purification of indoor air as reported by Agrios and Pichat [187]. Titanium dioxide can be used for both VOCs mineralization and bacterial disinfection, upon the addition of silver nanoparticles [188]. This acts as indoor-light-activated photocatalyst and prevents bacterial growth on the surface when used in tiles. The antibacterial action of nanocrystalline ZnS is compared with Evonik-Degussa P-25 as indoor-light-activated photocatalyst [189] to prevent bacterial growth on the surface.

Indoor air treatment usually takes place in an apparatus through which air is circulated. Such systems, which proceed through the following sequence of reactions, contain a blower or an air pump, a particulates filter or an electrostatic precipitator, and a light source and a photocatalyst.

$$\text{Contaminated air} \rightarrow A \rightarrow B \rightarrow C \rightarrow D \rightarrow E \rightarrow \text{purified air}$$

where A, B, C, D, and E, respectively, represent fan, particulates filter, photocatalyst, light source, and activated carbon filter (optional).

The drawback of this indoor air treatment is the formation of by-products that blocks active sites.

The basic concept in outdoor air treatment is to use a large area of construction as walls, roofs, roads, pavements, bridges, and buildings as platforms for air decontamination. The photocatalyst can be applied in various forms including cementitious modules, *in-situ*-made concrete objects, and over-coated thin layers. Outdoor air treatment differs from indoor air treatment by the type of contaminants (less VOCs and more NO_x, CO, and SO_x), by the use of solar light as the dominant irradiation source; by the fact that photocatalytic platforms are to serve for construction (unlike indoor air treatment devices designed for air cleaning); by the exposure to harsh environment; and by their visibility to general public. The number of gas-phase pollutants whose photocatalytic degradation has been studied is quite large. Some of these pollutants such as aromatic compounds, chlorinated olefins, hydrocarbons [190], aldehydes [191], and alcohols [192] can be found indoor. Nitrogen oxides (NO_x)

released mainly from internal combustion engines and furnaces can be reduced upon immobilizing TiO_2 on activated carbon [193,194]. Here, nitrogen oxides are oxidized to HNO_3 and washed away by rainfall when the catalyst is used outdoors. The use of zeolite matrix hosting TiO_2 may lead to the formation of ecofriendly products like N_2 and O_2 instead of nitric acid [195]. The oxidation of acetone, however, leads to the formation of H_2O and CO_2 as the by-products (Eq. (39)).

$$CH_3COCH_3 + 4O_2 \rightarrow 3CO_2 + 3H_2O \tag{39}$$

Treatment of polluted air streams is often more efficient than that of waste water streams. Here, gas-phase reactions occur faster than liquid-phase reactions. In the process of treating air streams, TiO_2 must be suspended on some short of surface to allow the gas to pass over it and react. This may be some short of matrix with a large surface area illuminated by UV light. An air treatment system for ethylene removal has been developed at University of Wisconsin-Madison [196]. This system can be placed in grocery stores to remove the naturally occurring ethylene that causes fruits and vegetables to spoil. Moreover, UV light reduces bacteria, molds, and odors. The mechanism in oxidizing pollutants arises from highly oxidizing hydroxyl radicals produced on the catalyst surface.

Carbon-doped TiO_2 has been used to investigate the PCO of toluene, a common VOC emitted by many industrial processes in air [197]. This C-doped TiO_2 has been synthesized by a sol–gel combustion method using carbon nano power. A nitrogen-doped and platinum-modified TiO_2 ($Pt/TiO_{2-x}N_x$) photocatalyst is proven effective for the decomposition of benzene and other persistent VOCs under visible-light irradiation in a $H_2{-}O_2$ atmosphere [198]. Ethyl benzene and o-, m-, and p-xylenes are removed by employing $N–TiO_2$ at indoor air level. Composite $N–TiO_2$/zeolite has been investigated for the removal of toluene from waste gas [199].

5.3. Hydrogen production

Photocatalytic water splitting using TiO_2 in the presence of solar light for hydrogen production offers a promising way for clean, low-cost environmentally friendly production of hydrogen. Presently, the efficiency of this water-splitting technology for hydrogen production is very low due to various factors. The main barriers are as usual the rapid recombination of photo-generated electron-hole pairs, backward reactions, and poor activation of TiO_2 by visible light. Many investigators have tried to overcome these barriers by modification technologies like metal loading, metal ion doping, dye sensitization, composite semiconductor, anion doping, and metal ion implantation. Now a days, a growing interest in hydrogen production using solar energy and water draws attention as water could be split (simultaneously oxidized and reduced to form O_2 and H_2, respectively) in a photoelectrochemical cell upon illuminating a TiO_2-single crystal photoanode and having an inert cathode to which a small electrochemical bias has been applied [200,201]. However, from the view point of H_2 production, it is not very attractive due to the position of its conduction band edge with respect to the redox potential of H_2/H_2O couple and its low visible-light absorption [18,202]. Splitting of water to produce hydrogen can be explained with the help of following reactions:

$$TiO_2 + hv \rightarrow e^-_{CB} + h^+_{vb} \tag{2}$$

At TiO_2 electrode:

$$H_2O + 2h^+ \rightarrow 1/2\ O_2 + 2H^+ \tag{40}$$

At platinum electrode:

$$2H^+ + 2e^- \rightarrow H_2 \tag{41}$$

Thus, the overall reaction is:

$$H_2O + 2hv \rightarrow 1/2\ O_2 + H_2 \tag{42}$$

For hydrogen production, the CB level should be more negative than hydrogen production level (E_{H_2/H_2O}), while the VB should be more positive than water oxidation level (E_{O_2/H_2O}) for efficient oxygen production from water by photocatalysis. The photocatalytic hydrogen production by TiO_2 is shown in Fig. 10.

Dye sensitization is widely used to utilize visible light for energy conversion. Under illumination by visible light, the excited dyes can inject electrons to CB of semiconductors to initiate the catalytic reactions as illustrated in Fig. 8. Higher hydrogen production rate can be obtained by efficient absorption of visible light. To obtain higher efficiency of hydrogen production using absorbed light, fast electron injection and slow backward reaction are required. Based on the literature on electron/hole recombination of dyes, the recombination times were found to be mostly in the order of nanoseconds to microseconds, sometimes in milliseconds [203–205], while the electron injection

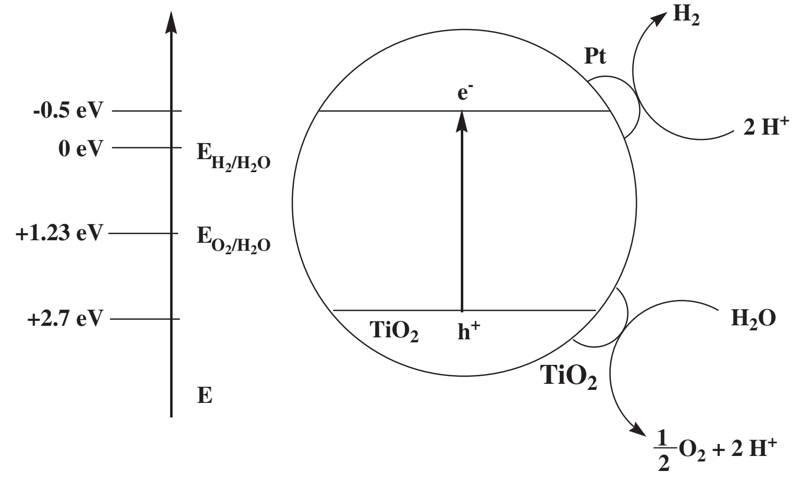

Fig. 10. Simplified mechanism of TiO_2 photocatalytic water splitting showing photo-excited electrons used for hydrogen production at platinum electrode.

times were in the order of femtoseconds [204,206,207]. The fast electron injection and slow backward reaction make dye-sensitized semiconductors feasible for efficient transfer of electrons from excited dyes to the CB of TiO_2. Dhanalakshmi et al. [208] carried out a parametric investigation to study the effect of using $[Ru(dcbpy)_2(dpd)]^{2+}$ [where dcbpy = 4,4-dicarboxy2,2-bipyridine and dpq = 2,3-bis-(2-pyridyl)-quinoxaline] as a dye sensitizer on photocatalytic hydrogen production from water, under visible-light irradiation. It was found that hydrogen production rate was enhanced by adsorbing dye molecules to TiO_2. Semiconductor composition (coupling) is another method to utilize visible light for hydrogen production. When a large band-gap semiconductor is coupled with a small band-gap semiconductor with a more negative CB level, CB electrons can be injected from the small band-gap semiconductor to the large band-gap semiconductor. Thus, a wide electron-hole separation is achieved as shown in Fig. 7. The process is similar to dye sensitization. The difference is that electrons are injected from one semiconductor to another semiconductor, rather than from excited dye to semiconductor. Successful coupling of the two semiconductors for photocatalytic water-splitting hydrogen production under visible-light irradiation can be achieved when the following conditions are met: (i) semiconductors should be free of photocorrosion; (ii) the small band gap semiconductor should be able to be excited by visible light; (iii) the CB of the small band-gap semiconductor should be more negative than that of the large band-gap semiconductor; (iv) the CB of the large band gap semiconductor should be more negative than E_{H_2/H_2O}; and (v) electron injection should be fast as well as efficient. There are reports of photocatalytic hydrogen production using CdS–TiO_2 composite semiconductors [209] and CdS–ZnS composite semiconductor [210,211].

6. Conclusion

This review focuses and reports the recent advances in the heterogeneous photocatalysis involving TiO_2 which can be used for the degradation and mineralization of various OCs found in water and air and for hydrogen production. A number of modification technologies, such as metal ion doping and metal ion implantation, nonmetal doping, dye sensitization, and composite semiconductor, are promising methods to expand light response of TiO_2 to visible region.

In spite of extensive investigations, the commercial exploitation of photocatalysis has not been done significantly. The application of this technique for real wastewaters and water purification for drinking purpose needs further investigation. Much research is needed to achieve stable pollutant removal through the optimization of process parameters and then only this technique would make a significant impact on the potential commercial and industrial application in water treatment. While the advances in TiO_2 photocatalysis using doped materials have been tested for relatively simple and clean solutions, the sustainability of their photocatalytic activity in real wastewaters is unclear which essentially requires further attention. On the technical point of view, the development of a more reliable and low-cost photocatalyst that can be activated by visible and solar light, or both, should be explored further for the potential application in water treatment. A comparison between water and air treatment reveals that the number of scientific publications on air treatment is significantly lower than that on water treatment. But, there is a growing interest to apply TiO_2 PCO process for air-cleaning as pollution level is growing day by day. In photocatalytic water splitting, efficient hydrogen production is possible by coupling different techniques. For example, when dye-sensitized TiO_2 loaded by noble metal is coupled with redox mediator, sustainable hydrogen is produced under solar irradiation.

This is important to note that mechanistic understanding about heterogeneous photocatalytic reactions is yet to achieve due to their complex nature. More effort is needed to explore complex mechanism of photocatalytic reactions. The current status of knowledge suggests that the mechanisms in photocatalytic reactions are difficult to generalize. It should be understood on a case-by-case basis. Although pure TiO_2 is a reasonably good photocatalyst, a variety of methods have been employed to improve its efficiency and overcome inactivity in the visible-light region. To conclude, it is hoped that very efficient modified TiO_2 photocatalysts will be developed for successful commercialization and especially for water treatment.

Acknowledgments

The authors gratefully acknowledge the University Grants Commission, Govt. of India for financial assistance (F. 40-76/2011 (SR)). The authors wish to acknowledge Mr. Bhauk Sinha and Mr. Morten Marbaniang for their help in the preparation of the manuscript.

References

[1] RA, Al-Rasheed, Water treatment by heterogeneous photocatalysis: An overview. Proceedings of the Fouth SWCC Acquired Experience Symposium: Jeddah, Al-Jubail, 2005.

[2] P.R. Gogate, A.B. Pandit, A review of imperative technologies for wastewater treatment I: Oxidation technologies at ambient conditions, Adv. Environ. Res. 8 (2004) 501–551.

[3] J.M. Herrmann, Heterogeneous photocatalysis: Fundamentals and applications to the removal of various types of aqueous pollutants, Catal. Today 53 (1999) 115–129.

[4] R. Andreozzi, V. Caprio, A. Insola, G. Longo, V. Tufano, Photocatalytic oxidation of 4-nitrophenol in aqueous TiO_2 slurries: An experimental validation of literature kineticmodels, J. Chem. Technol. Biotechnol. 75 (2000) 131–136.

[5] N.A. Laoufi, D. Tassalit, F. Bentahar, The degradationof phenol in water solution by TiO_2 photocatalysis in a helical reactor, Global Nest J. 10 (2008) 404–418.

[6] A. Fujishima, K. Honda, Electrochemical photolysis of water at a semiconductor electrode, Nature 37 (1972) 238–245.

[7] N. Miranda-García, S. Suárez, B. Sánchez, J.M. Coronado, S. Malato, M. Ignacio Maldonado, Photocatalytic degradation of emerging contaminants in municipal wastewater treatment plant effluents using immobilized TiO_2 in a solar pilot plant, Appl. Catal. B: Environ. 103 (2011) 294–301.

[8] M. Fane, TiO_2/AC composites for synergistic adsorption-photocatalysis processes: Present challenges and further developments for water treatment and reclamation, Crit. Rev. Environ. Sci. Technol. 41 (2011) 1173–1230.

[9] C.-H. Chiou, R.-S. Juang, Photocatalytic degradation of phenol in aqueous solutions by Pr-doped TiO_2 nanoparticles, J. Hazard. Mater. 149 (2007) 1–7.

[10] P. Wang, T. Zhou, R. Wang, T.-T. Lim, Carbon-sensitized and nitrogen-doped TiO_2 for photocatalytic degradation of sulfanilamide under visible-light irradiation, Water Res. 45 (2011) 5015–5026.

[11] Y.Y. Gurkan, N. Turkten, A. Hatipoglu, Z. Cina, Photocatalytic degradation of cefazolin over N-doped TiO_2 under UV and sunlight irradiation: Prediction of the reaction paths via conceptual DFT, Chem. Eng. J. 184 (2012) 113–124.

[12] C.C. Wong, W. Chu, The direct photolysis and photocatalytic degradation of alachlor at different TiO_2 and UV sources, Chemosphere 50 (2003) 981–987.

[13] B.K. Avasarala, S.R. Tirukkovalluri, S. Bojja, Photocatalytic degradation of monocrotophos pesticide—an endocrine disruptor by magnesium doped titania, J. Hazard. Mater. 186 (2011) 1234–1240.

[14] S.K. Sharma, H. Bhunia, P.K. Bajpai, Photocatalytic decolorization kinetics and adsorption isotherms of a mixture of two anionic azo dyes: Reactive red 120 and reactive black 5, Desalin. Water Treat. 44 (2012) 261–268.

[15] T. Visa, M. Sánchez, V. López-Grimau, R. Navarro, S. Reche, M.C. Gutiérrez-Bouzán, Photocatalysis with titanium dioxide to remove colour of exhausted reactive dyebaths without pH modification, Desalin. Water Treat. 45 (2012) 91–99.

[16] S.R. Patil, U.G. Akpan, B.H. Hameed, S.K. Samdarshi, A comparative study of the photocatalytic efficiency of Degussa P25, Qualigens, and Hombikat UV-100 in the degradation kinetic of congo red dye, Desalin. Water Treat. 46 (2012) 188–195.

[17] N. Meng, M.K.H. Leung, D.Y.C. Leung, K. Sumathy, A review and recent developments in photocatalytic water-splitting using TiO_2 for hydrogen production, Ren. Sust. Energy Rev. 11 (2007) 401–425.

[18] A. Fujishima, T.N. Rao, D.A. Tryk, Titanium dioxide photocatalysis, J. Photochem. Photobiol. C: Photochem. Rev. 1 (2000) 1–21.

[19] O. Carp, C.L. Huisman, A. Reller, Photoinduced reactivity of titanium dioxide, Prog. Solid State Chem. 32 (2004) 33–177.

[20] I.K. Konstantinou, V.A. Sakkas, T.A. Albanis, Photocatalytic degradation of propachlor in aqueous TiO_2 suspensions. Determination of the reaction pathway and identification of intermediate products by various analytical methods, Water Res. 36 (2002) 2733–2742.

[21] S. Sakthivel, B. Neppolian, M.V. Shankar, B. Arabindoo, M. Palanichamy, V. Murugesan, Solar photocatalytic degradation of azo dye: Comparison of photocatalytic efficiency of ZnO and TiO_2, Sol. Energy Mater. Sol. Cells 77 (2003) 65–82.

[22] A. Fujishima, K. Honda, K. Kohayakawa, Hydrogen production under sunlight with an electrochemical photocell, J. Electrochem. Soc. 122 (1975) 1487–1489.

[23] K.J. Hartig, N. Getoff, Optimization of n-TiO_2 films as photoanodes for water splitting, Proceedings of the Third International Congress on Hydrogen Materials, vol. 2, Paris, 1982, pp. 947–952.

[24] B. Ohtani, O.O. Prieto-Mahaney, D. Li, R. Abe, What is Degussa (Evonik) P25? Crystalline composition analysis, reconstruction from isolated pure particles and photocatalytic activity test J. Photochem. Photobiol. A: Chem. 216 (2010) 179–182.

[25] D. Duonghong, E. Borgarello, M. Grätzel, Dynamics of light-induced water cleavage in colloidal systems, J. Am. Chem. Soc. 103 (1981) 4685–4690.

[26] A. Mills, R.H. Davis, D. Worsley, Water purification by semiconductor photocatalysis, Chem. Soc. Rev. 22 (1993) 417–434.

[27] K. Hustert, R.G. Zepp, Photocatalytic degradation of selected azo dyes, Chemosphere 24 (1992) 335–342.

[28] R.J. Davis, J.L. Gainer, G. O'Neal, I. Wu, Photocatalytic decolorization of wastewater dyes, Water Environ. Res. 66 (1994) 50–53.

[29] M.S.T. Goncalves, A.M.F. Oliveira-Campos, E.M.M.S. Pinto, P.M.S. Plasência, M.J.R.P. Queiroz, Photochemical treatment of solutions of azo dyes containing TiO_2, Chemosphere 39 (1999) 781–786.

[30] C. Hu, Y. Wang, Decolorization and biodegradation of photocatalytic treated azo dyes and wool textile wastewater, Chemosphere 39 (1999) 2107–2115.

[31] K. Tanaka, K. Padermpole, T. Hisanaga, Photocatalytic degradation of commercial azo dyes, Water Res. 34 (2000) 327–333.

[32] N. Sobana, M. Swaminathan, The effect of operational parameters on the photocatalytic degradation of acid red 18 by ZnO, Sep. Purif. Technol. 56 (2007) 101–107.

[33] J. Domenech, A. Prieto, Stability of ZnO particles in aqueous suspensions under UV illumination, J. Phys. Chem. 90 (1986) 1123–1126.

[34] E.G. López, G. Marcí, N. Serpone, H. Hidaka, Photoassisted oxidation of the recalcitrant cyanuric acid substrate in aqueous ZnO suspensions, J. Phys. Chem. C 111 (2007) 18025–18032.

[35] N. Daneshvar, M.H. Rasoulifard, A.R. Khataee, F. Hosseinzadeh, Removal of C.I. acid orange 7 from aqueous solution by UV irradiation in the presence of ZnO nanopowder, J. Hazard. Mater. 143 (2007) 95–101.

[36] I.T. Peternel, N. Koprivanac, A.M.L. Božić, H.M. Kušić, Comparative study of UV/TiO_2, UV/ZnO and photo-Fenton processes for the organic reactive dye degradation in aqueous solution, J. Hazard. Mater. 148 (2007) 477–484.

[37] R.A. Palominos, M.A. Mondaca, A. Giraldo, G. Peñuela, M. Pérez-Moya, H.D. Mansilla, Photocatalytic oxidation of the antibiotic tetracycline on TiO_2 and ZnO suspensions, Catal. Today 144 (2009) 100–105.

[38] B. Swarnalatha, Y. Anjaneyulu, Studies on the heterogeneous photocatalytic oxidation of 2, 6-dinitrophenol in aqueous TiO_2 suspension, J. Mol. Catal. A: Chem. 223 (2004) 161–165.

[39] P. Ji, J. Zhang, F. Chen, M. Anpo, Ordered mesoporous CeO_2 synthesized by nanocasting from cubic la 3d mesoporous MC-48 silica: Formation, characterization and photocatalytic activity, J. Phys. Chem. C 112 (2008) 17809–17813.

[40] C.-F. Lin, C.-H. Wu, Z.-N. Onn, Degradation of 4-chlorophenol in TiO_2, WO_3, SnO_2, TiO_2/WO_3 and TiO_2/SnO_2 systems, J. Hazard. Mater. 154 (2008) 1033–1039.

[41] G. Al-Sayyed, J.C. D'Oliverira, P. Pichat, Semiconductorsensitized photodegradation of 4-chlorophenol in water, J. Photochem. Photobiol. A: Chem. 58 (1991) 99–114.

[42] V. Augugliaro, L. Palmisano, M. Schiavello, A. Sclafani, L. Marchese, G. Martra, J. Miano, Photocatalytic degradation of nitrophenols in aqueous titanium dioxide dispersion, Appl. Catal. 69 (1991) 323–340.

[43] M.R. Hoffmann, S.T. Martin, W. Choi, D.W. Bahnemann, Environmental applications of semiconductor photocatalysis, Chem. Rev. 95 (1995) 69–96.

[44] D. Lawless, N. Serpone, D. Meisel, Role of hydroxyl radicals and trapped holes in photocatalysis. A pulse radiolysis study, J. Phys. Chem. 95 (1991) 5166–5170.

[45] S. Irmak, E. Kusvuran, O. Erbatur, Degradation of 4-chloro-2-methylphenol in aqueous solution by UV irradiation in the presence of titanium dioxide, Appl. Catal. B: Environ. 54 (2004) 85–91.

[46] L. Ravichandran, K. Selvam, M. Swaminathan, Effect of oxidants and metal ions on photodefluoridation of pentafluorobenzoic acid with ZnO, Sep. Purif. Technol. 56 (2007) 192–198.

[47] K. Selvam, M. Muruganandham, I. Muthuvel, M. Swaminathan, The influence of inorganic oxidants and metal ions on semiconductor sensitized photodegradation of 4-fluorophenol, Chem. Eng. J. 128 (2007) 51–57.

[48] A. Syoufian, K. Nakashima, Degradation of methylene blue in aqueous dispersion of hollow titania photocatalyst: Study of reaction enhancement by various electron scavengers, J. Colloid Interface Sci. 317 (2008) 507–512.

[49] N. Kashif, F. Ouyang, Parameters effectonheterogeneous photocatalysed degradation of phenol in aqueous dispersion of TiO_2, J. Environ. Sci. 21 (2009) 527–533.

[50] A.J. Hoffman, E.R. Carraway, M.R. Hoffmann, Photocatalytic production of H_2O_2 and organic peroxides on quantum-sized semiconductor collolds, Environ. Sci. Technol. 28 (1994) 776–785.

[51] C. Bernardini, G. Cappelletti, M.V. Dozzi, E. Selli, Photocatalytic degradation of organic molecules in water: Photoactivity and reaction paths in relation to TiO_2 particles features, J. Photochem. Photobiol. A: Chem. 211 (2010) 185–192.

[52] M. Mrowetz, E. Selli, Photocatalytic degradation of formic and benzoic acids and hydrogen peroxide evolution in TiO_2 and ZnO water suspensions, J. Photochem. Photobiol. A: Chem. 180 (2006) 15–22.

[53] S. Malato, J. Blanco, C. Richter, B. Braun, M.I. Maldonado, Enhancement of the rate of solar photocatalytic mineralization of organic pollutants by inorganic oxidizing species, Appl. Catal. B: Environ. 17 (1998) 347–356.

[54] I. Poulios, I. Aetopoulou, Photocatalytic degradation of the textile dye reactive orange 16 in the presence of TiO_2 suspensions, Environ. Technol. 20 (1999) 479–487.

[55] I. Poulios, I. Aetopoulou, Photodegradation of the textile dye reactive black in the presence of semiconducting oxides, J. Chem. Technol. Biotechnol. 74 (1999) 349–357.

[56] O. Legrini, E. Oliveros, A.M. Braun, Photochemical processes for water treatment, Chem. Rev. 93 (1993) 671–698.

[57] L. Dogliotti, E. Hayon, Flash photolysis of peroxydisulfate ions in aqueous solutions. The sulfate and ozonide radical anions, J. Phys. Chem. 71 (1967) 2511–2516.

[58] W.A. Sadik, Effect of inorganic oxidants in photodecolourization of an azo dye, J. Photochem. Photobiol. A: Chem. 191 (2007) 132–137.

[59] N. San, A. Hatipoglu, G. Koctürk, Z. Çınar, Photocatalytic degradation of 4-nitrophenol in aqueous TiO_2 suspensions: Theoretical prediction of the intermediates, J. Photochem. Photobiol. A: Chem. 146 (2002) 189–197.

[60] L.K. Weavers, I. Hua, M.R. Hoffmann, Degradation of triethanolamine and chemical oxygen demand reduction in wastewater by photoactivated periodate, Water Environ. Res. 69 (1997) 1112–1119.

[61] W.A. Sadik, O.M. Sadek, A.M. El-Demerdash, The use of heterogeneous advanced oxidation processes to degrade neutral red dye in aqueous solution, Polym. Plast. Technol. Eng. 43 (2004) 1675–1686.

[62] Y. Wang, C.-S. Hong, Effect of hydrogen peroxide, periodate and persulfate on photocatalysis of 2-chlorobiphenyl in aqueous TiO_2 suspensions, Water Res. 33 (1999) 2031–2036.

[63] C. Lee, J. Yoon, Application of photoactivated periodate to the decolorization of reactive dye: Reaction parameters and mechanism, J. Photochem. Photobiol. A: Chem. 165 (2004) 35–41.

[64] B. Gözmen, M. Turabik, A. Hesenov, Photocatalytic degradation of basic red 46 and basic yellow 28 in single and binary mixture by UV/TiO_2/periodate system, J. Hazard. Mater. 164 (2009) 1487–1495.

[65] C.G. da Silva, J.L. Faria, Photochemical and photocatalytic degradation of an azo dye in aqueous solution by UV irradiation, J. Photochem. Photobiol. A: Chem. 155 (2003) 133–143.

[66] N. San, A. Hatipoglu, G. Koctürk, Z. Cinar, Prediction of primary intermediates and the photodegradation kinetics of 3-aminophenol in aqueous TiO_2 suspensions, J. Photochem. Photobiol. A: Chem. 139 (2001) 225–232.

[67] D.S. Bhatkhande, V.G. Pangarkar, A.A.C.M. Beenackers, Photocatalytic degradation for environmental applications—A review, J. Chem. Technol. Biotechnol. 77 (2002) 102–116.

[68] S.P. Kamble, S.B. Sawant, V.G. Pangarkar, Photocatalytic degradation of m-nitrobenzenesulfonic acid using solar and artificial UV radiation, J. Chem. Technol. Biotechnol. 81 (2006) 359–3364.

[69] S. Teekateerawej, J. Nishino, Y. Nosaka, Design and evaluation of photocatalytic micro-channel reactors using TiO_2-coated porous ceramics, J. Photochem. Photobiol. A: Chem. 179 (2006) 263–268.

[70] O.M. Alfano, D. Bahnemann, A.E. Cassano, R. Dillert, R. Goslich, Photocatalysis in water environments using artificial and solar light, Catal. Today 58(2–3) (2000) 199–230.

[71] M.S. Vohra, K. Tanaka, Enhanced photocatalytic activity of nafion-coated TiO_2, Environ. Sci. Technol. 35 (2001) 411–415.

[72] C. Kormann, D.W. Bahnemann, M.R. Hoffmann, Preparation and characterization of quantum-size titanium dioxide, J. Phys. Chem. 92 (1988) 5196–5201.

[73] Y. Xu, M.A.A. Schoonen, The absolute energy position of conduction and valence bands of selected semiconducting minerals, Am. Mineral. 85 (2000) 543–556.

[74] A.R. Doong, C.H. Chen, R.A. Maithreepala, S.M. Chang, The influence of pH and cadmium sulphide on the photocatalytic degradation of 2-chlorophenol in titanium dioxide suspensions, Water Res. 35 (2001) 2873–2880.

[75] K. Pujara, S.P. Kamble, V.G. Pangarkar, Photocatalytic degradation of phenol-4-sulfonic acid using an artificial UV/TiO_2 system in a slurry bubble column reactor, Ind. Eng. Chem. Res. 46 (2007) 4257–4264.

[76] H.Y. Chen, O. Zahraa, M. Bouchy, Inhibition of the adsorption and photocatalytic degradation of an organic contaminant in an aqueous suspension of TiO_2 by inorganic ions, J. Photochem. Photobiol. A: Chem. 108 (1997) 37–44.

[77] O.V. Makarova, T. Rajh, M.C. Thurnauer, A. Martin, P.A. Kemme, D. Cropek, Surface modification of TiO_2 nanoparticles for photochemical reduction of nitrobenzene, Environ. Sci. Technol. 34 (2000) 4797–4803.

[78] D. Zhao, C.C. Chen, Y. Wang, H. Ji, W. Ma, L. Zang, J. Zhao, Surface modification of TiO_2 by phosphate: Effect on photocatalytic activity and mechanism implication, J. Phys. Chem. C 112 (2008) 5993–6001.

[79] V. Subramanian, V.G. Pangarkar, A.A.C.M. Beenackers, Photocatalytic degradation of para-hydroxybenzoic acid: Relationship between substrate adsorption and photocatalytic degradation, Clean Prod. Processes 2 (2000) 149–156.

[80] A.A. Yawalkar, D.S. Bhatkhande, V.G. Pangarkar, A.A.C.M. Beenackers, Solar assisted photocatalytic and photochemical degradation of phenol, J. Chem. Technol. Biotechnol. 76 (2001) 363–370.

[81] R.-J. Wu, C.-C. Chen, C.-S. Lu, P.-Y. Hsu, M.-H. Chen, Phorate degradation by photocatalysis: Parameter and reaction pathway investigations, Desalination 250 (2010) 869–875.

[82] S.P. Kamble, S.B. Sawant, V.G. Pangarkar, Photocatalytic and photochemical degradation of aniline using concentrated solar radiation, J. Chem. Technol. Biotechnol. 78 (2003) 865–872.

[83] T.-Y. Wei, C.-C. Wan, Kinetics of photocatalytic oxidation of phenol on surface, Kinetics of photocatalytic oxidation of phenol on TiO_2 surface 69 (1992) 241–249.

[84] Y.T. Wei, Y.Y. Wang, C. Wan, Photocatalytic oxidation of phenol in the presence of hydrogen peroxide and titanium dioxide powders, J. Photochem. Photobiol. A: Chem. 55 (1990) 115–126.

[85] A. Sclafani, L. Palmisano, E. Devi, Photocatalytic degradaton of phenol in aqueous polycrystalline TiO_2 dispersions: The influence of Fe^{3+}, Fe^{2+} and Ag^+ on the reaction rate, J. Photochem. Photobiol. A: Chem. 56 (1991) 113–123.

[86] M. Bideau, B. Claudel, L. Faure, H. Kazaoun, The photo-oxidation of acetic acid by oxygen in the presence of titanium dioxide and dissolved copper ions, J. Photochem. Photobiol. A: Chem. 61 (1991) 269–280.

[87] E.C. Butler, A.P. Davis, Photocatalytic oxidation in aqueous titanium dioxide suspensions: The influence of dissolved transition metals, J. Photochem. Photobiol. A: Chem. 70 (1993) 273–283.

[88] N.S. Foster, R.D. Noble, C.A. Koval, Reversible photoreductive deposition and oxidative dissolution of copper ions in titanium dioxide aqueous suspensions, Environ. Sci. Technol. 27 (1993) 350–356.

[89] E.T. Soares, M.A. Lansarin, C.C. Moro, A study of process variables for the photocatalytic degradation of rhodamine b, Braz. J. Chem. Eng. 24 (2007) 29–36.

[90] Q. Hu, B. Liu, Z. Zhang, M. Song, X. Zhao, Temperature effect on the photocatalytic degradation of methyl orange under UV–vis light irradiation, J. Wuhan Univ. Technol. Mater. Sci. Ed. 25 (2010) 210–213.

[91] J.-M. Herrmann, Heterogeneous photocatalysis: State of the art and present applications in honor of Pr R.L. Burwell Jr. (1912–2003), Former Head of Ipatieff Laboratories, Northwestern University, Evanston (Ill), Top. Catal. 34 (2005) 49–65.

[92] N. Barka, S. Qourzal, A. Assabbane, A. Nounah, Y. Ait-Ichou, Photocatalytic degradation of patent blue V by supported TiO_2: Kinetics, mineralization, and reaction pathway, Chem. Eng. Commun. 198 (2011) 1233–1243.

[93] P.-S. Yap, T.-T. Lim, Effect of aqueous matrix species on synergistic removal of bisphenol-A under solar irradiation using nitrogen-doped TiO_2/AC composite, Appl. Catal. B: Environ. 101 (2011) 709–717.

[94] L. Rizzo, S. Meric, D. Kassinos, M. Guida, F. Russo, V. Belgiorno, Degradation of diclofenac by TiO_2 photocatalysis: UV absorbance kinetics and process evaluation through a set of toxicity bioassays, Water Res. 43 (2009) 979–988.

[95] M. Sanchez, M.J. Rivero, I. Ortiz, Kinetics of dodecylbenzenesulphonate mineralisation by TiO_2 photocatalysis, Appl. Catal. B: Environ. 101 (2011) 515–521.

[96] M. El-Kemary, H. El-Shamy, Fluorescence modulation and photodegradation characteristics of safranin O dye in the presence of ZnS nanoparticles, J. Photochem. Photobiol. A: Chem. 205 (2009) 151–155.

[97] Z. He, T. Hong, J. Chen, S. Song, A magnetic TiO_2 photocatalyst doped with iodine for organic pollutant degradation, Sep. Purif. Technol. 96 (2012) 50–57.

[98] N. Serpone, Is the band gap of pristine TiO_2 narrowed by anion- and cation-doping of titanium dioxide in second-generation photocatalysts? J. Phys. Chem. B. 110 (2006) 24287–24293.

[99] B. Sun, A.V. Vorontsov, P.G. Smirniotis, Role of platinum deposited on titania during phenol photocatalytic oxidation, Langmuir 19 (2003) 3151–3156.

[100] M. Franch, J. Peral, X. Domenech, J.A. Ayllon, Aluminium (III) adsorption: A soft and simple method to prevent TiO_2 deactivation during salicylic acid photodegradation, Chem. Commun. 14 (2005) 1851–1853.

[101] A. Di Paola, G. Marci, L. Palmisano, M. Schiavello, K. Upsali, S. Ikeda, Preparation of polycrystalline TiO_2 photocatalysts impregnated with various transition metal ions: Characterization and photocatalytic activity for the degradation of 4-nitrophenol, J. Phys. Chem. B 106 (2002) 637–645.

[102] Y. Cao, W. Yang, W. Zhang, G. Liu, P. Yue, Improved photocatalytic activity of Sn^{4+} doped TiO_2 nanoparticulate films prepared by plasma-enhanced chemical vapor deposition, New J. Chem. 28 (2004) 218–222.

[103] Q. Liu, X. Wu, B. Wang, Q. Liu, Preparation and superhydrophilic properties of TiO_2/SnO_2 composite thin films, Mater. Res. Bull. 37 (2002) 2255–2262.

[104] V. Subramanian, E. Wolf, P.V. Kamat, Semiconductor-metal composite nanostructures. To what extent do metal nanoparticles improve the photocatalytic activity of TiO_2 films? J. Phys. Chem. B 105 (2001) 11439–11446.
[105] C. Lettmann, H. Hinrichs, W.F. Maier, Combinatorial discovery of new photocatalysts for water purification with visible light, Angew. Chem. 40 (2001) 3160–3163.
[106] S. Girish Kumar, L. Gomathi Devi, Review on modified TiO_2 photocatalysis under UV–visible light: Selected results and related mechanisms on interfacial charge carrier transfer dynamics, J. Phys. Chem. A 115 (2011) 13211–13241.
[107] J.A. Pedraza-Avella, R. López, F. Martínez-Ortega, E.A. Páez-Mozo, R. Gómez, Effect of chromium doping on visible light absorption of nanosized titania sol–gel, J. Nano Res. 5 (2009) 95–104.
[108] J. Chen, X.Y.M. Wang, Investigation of transitionmetal ion doping behaviors on TiO_2 nanoparticles, J. Nanopart. Res. 10 (2008) 163–171.
[109] S.D. Sharma, D. Singh, K.K. Saini, C.H. Kant, V. Sharma, S. C. Jain, Sol–gel derived super-hydrophilic nickel doped TiO_2 film as active photo-catalyst, Appl. Catal. A: Gen. 314 (2006) 40–46.
[110] J.C.S. Wu, C.H. Chen, A visible-light response vanadium-doped titania nanocatalyst by sol–gel method, J. Photochem. Photobiol. A: Chem. 163 (2004) 509–515.
[111] K.T. Ranjit, B. Viswanathan, Photocatalytic properties of iron-doped titania semiconductors, J. Photochem. Photobiol. A: Chem. 108 (1997) 79–84.
[112] M.I. Litter, J.A. Navigo, Photocatalytic properties of iron-doped titania semiconductors, J. Photochem. Photobiol. A: Chem. 98(3) (1996) 171–181.
[113] J.A. Navigo, G. Colon, M. Macias, C. ReL, M.I. Litter, Iron-doped titania semiconductor powders prepared by a sol–gel method. Part I: Synthesis and characterization, Appl. Catal. A: Gen. 177 (1999) 111–120.
[114] M. Tomkiewicz, Scaling properties in photocatalysis, Catal. Today 58 (2000) 115–123.
[115] K. Mizushima, M. Tanaka, A. Asai, S. Lida, J. Goodenough, Impurity levels of iron-group ions in TiO_2, J. Phys. Chem. Solids 40 (1979) 1129–1140.
[116] J.A. Navio, J.J. Testa, P. Djedjeian, J.R. Padron, D. Rodriguez, M.I. Litter, Irondoped titania powders prepared by a sol–gel method: Part II: Photocatalytic properties, Appl. Catal. A: Gen. 178(2) (1999) 191–203.
[117] M. Asilturk, F. Sayilkan, E. Arpac, Effect of Fe^{3+} ion doping to TiO_2 on the photocatalytic degradation of Malachite green dye under UV and vis-irradiation, J. Photochem. Photobiol. A: Chem. 203 (2009) 64–71.
[118] M.A. Behnajady, N. Modirshahla, M. Shokri, B. Rad, Enhancement of photocatalytic activity of TiO_2 nanoparticles by silver doping: Photodepositionversus liquid impregnation methods, Global Nest J. 10 (2008) 1–7.
[119] M.K. Seery, R. George, P. Floris, S.C. Pillai, Silver doped titanium dioxide nanomaterials for enhanced visible light photocatalysis, J. Photochem. Photobiol. A: Chem. 189 (2007) 258–263.
[120] C. Sahoo, A.K. Gupta, A. Pal, Photocatalytic degradation of crystal violet (C.I. basic violet 3) on silver ion doped TiO_2, Dyes Pigm. 66 (2005) 189–196.
[121] J.-F. Guo, B. Ma, A. Yin, K. Fan, W.-L. Dai, Highly stable and efficient Ag/AgCl@TiO_2 photocatalyst: Preparation, characterization, and application in the treatment of aqueous hazardous pollutants, J. Hazard. Mater. 211–212 (2012) 77–88.
[122] I.M. Arabatzis, T. Stergiopoulos, D. Andreeva, S. Kitova, S. G. Neophytides, P. Falaras, Characterization and photocatalytic activity of Au/TiO_2 thin films for azo-dye degradation, J. Catal. 220 (2003) 127–135.
[123] F.B. Li, X.Z. Li, The enhancement of photodegradation efficiency using Pt–TiO_2 catalyst, Chemosphere 48 (2002) 1103–1111.
[124] D. Hufschmidt, D. Bahnemann, J.J. Testa, C.A. Emilio, M.I. Litter, Enhancement of the photocatalytic activity of various TiO_2 materials by platinisation, J. Photochem. Photobiol. A: Chem. 148 (2002) 223–231.
[125] M. Anpo, M. Takeuchi, The design and development of highly reactive titanium oxide photocatalysts operating under visible light irradiation, J. Catal. 216 (2003) 505–516.
[126] R. Gomathi, A. Geetha Maheswari, The design and development of highly reactive titanium oxide photocatalysts operating under visible light irradiation, J. Catal. 216 (2003) 505–516.
[127] S. Senthilkumaar, K. Porkodi, N. Manonmani, Sole-gel derived silver doped nanocrystalline titania catalysed photodegradation of methylene blue from aqueous solution, Dyes Pigm. 69 (2006) 22–30.
[128] M. Huang, C. Xu, Z. Wu, Y. Huang, J. Lin, J. Wu, Photocatalytic discolorization of methyl orange solution by Pt modified TiO_2 loaded on natural zeolite, Dyes Pigm. 77 (2008) 327–334.
[129] R. Asahi, T. Morikawa, T. Ohwaki, K. Aoki, Y. Taga, Visible-light photocatalysis in nitrogen-doped titanium oxides, Science 294 (2001) 269–271.
[130] H. Irie, Y. Watanabe, K. Hashimoto, Nitrogen-concentration dependence on photocatalytic activity of $TiO_{2-x}N_x$ powders, J. Phys. Chem. B 107 (2003) 5483–5486.
[131] T. Ihara, M. Miyoshi, Y. Iriyama, O. Matsumoto, S. Sugihara, Visible-light-active titanium oxide photocatalyst realized by an oxygen-deficient structure and by nitrogen doping, Appl. Catal. B 42(4) (2003) 403–409.
[132] T. Ohno, M. Akiyoshi, T. Umebayashi, K. Asai, T. Mitsui, M. Matsumura, Preparation of S-doped TiO_2 photocatalysts and their photocatalytic activities under visible light, Appl. Catal. A: Gen. 265 (2004) 115–121.
[133] T. Matsumoto, N. Iyi, Y. Kaneko, K. Kitamura, S. Ishihara, Y. Takasu, High visible-light photocatalytic activity of nitrogen-doped titania prepared from layered titania/isostearate nanocomposite, Catal. Today 120 (2007) 226–232.
[134] K. Kobayakawa, Y. Murakami, Y. Sato, Visible-light active N-doped TiO_2 prepared by heating of titanium hydroxide and urea, J. Photochem. Photobiol. A: Chem. 170 (2005) 177–179.
[135] R. Bacsa, J. Kiwi, T. Ohno, P. Albers, V. Nadtochenko, Preparation, testing and characterization of doped TiO_2 active in the peroxidation of biomolecules under visible light, J. Phys. Chem. B 109 (2005) 5994–6003.
[136] B.F. Abramović, D.V. Šojića, V.B. Anderluha, N.D. Abazovićb, M.I. Čomor, Nitrogen-doped TiO_2 suspensions in photocatalytic degradation of mecoprop and (4-chloro-2-methylphenoxy) acetic acid herbicides using various light sources, Desalination 244 (2009) 293–302.
[137] N.T. Nolan, D.W. Synnott, M.K. Seery, S.J. Hinder, A. Van Wassenhovend, S.C. Pillai, Effect of N-doping on the photocatalytic activity of sol–gel TiO_2, J. Hazard. Mater. 211–212 (2012) 88–94.
[138] M.V. Dozzi, E. Selli, Doping TiO_2 with p-block elements: Effects on photocatalytic activity, J. Photochem. Photobiol. C: Photochem. Rev. 14 (2013) 13–28.
[139] X. Yang, Ch. Cao, K. Hohn, L. Ericsson, R. Maghirang, D. Hamal, Highly visible-light active C- and V-doped TiO_2 for degradation of acetaldehyde, J. Catal. 252 (2007) 296–302.
[140] T. Matsunaga, M. Inagaki, Carbon-coated anatase for oxidation of methylene blue and NO, Appl. Catal. B: Environ. 64 (2006) 9–12.
[141] C. Lettmann, K. Hildenbrad, H. Kisch, W. Macyk, W.F. Maier, Visible light photodegradation of 4-chlorophenol with a coke-containing titanium dioxide photocatalyst, Appl. Catal. B: Environ. 32 (2001) 215–227.
[142] J. Matos, A. Garcia, L. Zhao, M.M. Titirici, Solvothermal carbon-doped TiO_2 photocatalyst for the enhanced methylene blue degradation under visible light, Appl. Catal. A: Gen. 390 (2010) 175–182.

[143] E.K. Nejman, M. Janus, B. Grzmil, A.W. Morawski, Methylene blue decomposition under visible light irradiation in the presence of carbon-modified TiO_2 photocatalysts, J. Photochem. Photobiol. A: Chem. 226 (2011) 68–72.

[144] E.M. Rockafellow, L.K. Stewart, W.S. Jenks, Is sulfur-doped TiO_2 an effective visible light photocatalyst for remediation? Appl. Catal. B: Environ. 91 (2009) 554–562.

[145] Y.Y. Gurkan, E. Kasapbasi, Z. Cinar, Enhanced solar photocatalytic activity of TiO_2 by selenium(IV) ion-doping: Characterization and DFT modeling of the surface, Chem. Eng. J. 214 (2013) 34–44.

[146] S. Sakthivel, M. Janczarek, H. Kisch, Visible light activity and photoelectrochemical properties of nitrogen-doped TiO_2, J. Phys. Chem. B 108 (2004) 19384–19387.

[147] C.D. Valentin, G. Pacchioni, A. Selloni, Theory of carbon doping of titanium dioxide, Chem. Mater. 17 (2005) 6656–6665.

[148] T. Tachikawa, Y. Takai, S. Tojo, M. Fujitsuka, H. Irie, K. Hashimoto, T. Majima, Visible light-induced degradation of ethylene glycol on nitrogen-doped TiO_2 powders, J. Phys. Chem. B 110 (2006) 13158–13165.

[149] F. Tian, C. Liu, DFT description on electronic structure and optical absorption properties of anionic S-doped anatase TiO_2, J. Phys. Chem. B 110 (2006) 17866–17871.

[150] H. Liu, A. Imanishi, Y. Nakato, Mechanisms for photooxidation reactions of water and organic compounds on carbon-doped titanium dioxide, as studied by photocurrent measurements, J. Phys. Chem. C 111 (2007) 8603–8610.

[151] R. Nakamura, T. Tanaka, Y. Nakato, Mechanism for visible light responses in anodic photocurrents at N-doped TiO_2 film electrodes, J. Phys. Chem. B 108 (2004) 10617–10620.

[152] K.M. Schindler, M. Kunst, Charge-carrier dynamics in TiO_2 powders, J. Phys. Chem. 94 (1990) 8222–8226.

[153] H. Huang, D. Li, Q. Lin, W. Zhang, Y. Shao, Y. Chen, M. Sun, X. Fu, Efficient degradation of benzene over $LaVO_4/TiO_2$ nanocrystalline heterojunction photocatalyst under visible light irradiation, Environ. Sci. Technol. 43 (2009) 4164–4168.

[154] S. Livraghi, M.C. Paganini, E. Giamello, A. Selloni, C. Di Valentin, G. Pacchioni, Origin of photoactivity of nitrogen-doped titanium dioxide under visible light, J. Am. Chem. Soc. 128 (2006) 15666–15671.

[155] E. Bae, W. Choi, Effect of the anchoring group (carboxylate vs. phosphonate) in Ru-complex-sensitized TiO_2 on hydrogen production under visible light, J. Phys. Chem. B 110 (2006) 14792–14799.

[156] J.B. Zhong, J.Z. Li, F.M. Feng, Y. Lu, J. Zeng, W. Hu, Z. Tang, Improved photocatalytic performance of SiO_2–TiO_2 prepared with the assistance of SDBS, J. Mol. Catal. A: Chem. 357 (2012) 101–105.

[157] B.-H. Xu, B.-Z. Lin, Q.-Q. Wang, X.-T. Pian, O. Zhang, L.-M. Fu, Anatase TiO_2-pillared hexaniobate mesoporous nanocomposite with enhanced photocatalytic activity, Microporous Mesoporous Mater. 147 (2012) 79–85.

[158] E. Palomares, J.N. Clifford, S.A. Haque, T. Luts, J.R. Durrant, Control of charge recombination dynamics in dye sensitized solar cells by the use of conformally deposited metal oxide blocking layers, J. Am. Chem. Soc. 125 (2003) 475–482.

[159] H. Choi, S. Kim, S.O. Kang, J. Ko, M.-S. Kang, J.N. Clifford, A. Forneli, E. Palomares, M.K. Nazeeruddin, M Gratzel, Stepwise cosensitization of nanocrystalline TiO_2 films utilizing Al_2O_3 layers in dye-sensitized solar cells, Angew. Chem. 47 (2008) 8259–8263.

[160] Y. Cong, J. Zhang, F. Chen, M. Anpo, D. He, Preparation, photocatalytic activity, and mechanism of nano-TiO_2 co-doped with nitrogen and iron (III), J. Phys. Chem. C 111 (2007) 10618–10623.

[161] E. Bae, W. Choi, J. Park, H.S. Shin, S.B. Kim, J.S. Lee, Effects of surface anchoring groups (carboxylate vs. phosphonate) in ruthenium-complex-sensitized TiO_2 on visible light reactivity in aqueous suspensions, J. Phys. Chem. B 108 (2004) 14093–14101.

[162] F. Chen, Z. Deng, X. Li, J. Zhang, J. Zhao, Visible light detoxification by 2,9,16,23-tetracarboxyl phthalocyanine copper modified amorphous titania, Chem. Phys. Lett. 415 (2005) 85–88.

[163] F. Chen, W. Zou, W. Qu, J. Zhang, Photocatalytic performance of a visible light TiO_2 photocatalyst prepared by a surface chemical modification process, Catal. Commun. 10 (2009) 1510–1513.

[164] H. Lachheba, O. Ahmed, A. Houas, J.P. Nogier, Photocatalytic activity of TiO_2-SBA-15 under UV and visible light, J. Photochem. Photobiol. A: Chem. 226 (2011) 1–8.

[165] W. Kim, T. Tachikawa, T. Majima, W. Choi, Photocatalysis of dye-sensitized TiO_2 nanoparticles with thin overcoat of Al_2O_3: Enhanced activity for H_2 production and dechlorination of $CClO_4$, J. Phys. Chem. C 113 (2009) 10603–10609.

[166] M. Pelaez, N.T. Nolan, S.C. Pillai, M.K. Seery, P. Falaras, A. G. Kontos, P.S.M. Dunlop, J.W.J. Hamilton, J.A. Byrne, K. O'Shea, M.H. Entezari, D.D. Dionysiou, A review on the visible light active titanium dioxide photocatalysts for environmental applications, Appl. Catal. B: Environ. 125 (2012) 331–349.

[167] M.R. Prairie, L.R. Evans, B.M. Stange, S.L. Martinez, An investigation of titanium dioxide photocatalysis for the treatment of water contaminated with metals and organic chemicals, Environ. Sci. Technol. 27 (1993) 1776–1782.

[168] K. Pirkanniemi, M. Sillanpää, Heterogeneous water phase catalysis as an environmental application: A review, Chemosphere 48 (2002) 1047–1060.

[169] D. de Bem Luiz, S.L.F. Andersen, C. Berger, H.J. Jose, M. Regina de Fatima Peralta Muniz, Photocatalytic reduction of nitrate ions in water over metal-modified TiO_2, J. Photochem. Photobiol. A: Chem. 246 (2012) 36–44.

[170] A. Vidol, A.I. Diaz, E.A. Hpiki, M. Romero, I.F. Muguruza, J. González, Solar photocatalysis for detoxification and disinfection of contaminated water: Pilot plant studies, Catal. Today 54 (1999) 283–290.

[171] D.M. Blake, Bibliography of work on the heterogeneous photocatalytic removal of hazardous compounds from water and air, Tech. Report, NREL, Colorado, 2001, pp. 1–158.

[172] D. Chen, A.K. Ray, Removal of toxic metal ions from wastewater by semiconductor photocatalysis, Chem. Eng. Sci. 56 (2001) 1561–1570.

[173] B. Czech, W. Ćwikła-Bundyra, Advanced oxidation processes in triton X-100 and wash-up liquid removal from wastewater using modified TiO_2/Al_2O_3 photocatalysts, Water Air Soil Pollut. 223(8) (2012) 4813–4822.

[174] T. Matsunaga, R. Tomoda, T. Nakajima, H. Wake, Photoelectrochemical sterilization of microbial cells by semiconductor powders, FEMS Microbiol. Lett. 29 (1985) 211–214.

[175] A. Mills, S.L. Hunte, An overview of semiconductor photocatalysis, J. Photochem. Photobiol. A: Chem. 108 (1997) 1–35.

[176] S. Malato, J. Blanco, D.C. Alarcón, M.I. Maldonado, P.F. Ibáñez, W. Gernjak, Photocatalytic decontamination and disinfection of water with solar collectors, Catal. Today 122 (2007) 137–149.

[177] S.P. Rémy, F. Simonet, E.E. Cerdad, J.C. Lazzaroni, D. Atlan, C. Guillard, Photocatalysis and disinfection of water: Identification of potential bacterial targets, Appl. Catal. B: Environ. 104 (2011) 390–398.

[178] G.S. Shephard, S. Stockenstrom, D. de Villiers, W.J. Engelbrecht, G.F.S. Wessels, Degradation of microcystin toxins in a falling film photocatalytic reactor with immobilized titanium dioxide catalyst, Water Res. 36 (2002) 140–146.

[179] M.A. Lazar, S. Varghese, S.S. Nair, Photocatalytic water treatment by titanium dioxide: Recent updates, Catalysts 2 (2012) 572–601.

[180] S. Malato, P.F. Ibáñez, M.I. Maldonado, J. Blanco, W. Gernjak, Decontamination and disinfection of water by solar photocatalysis: Recent overview and trends, Catal. Today 147 (2009) 1–59.

[181] O.K. Dalrymple, E. Stefanakos, M.A. Trotz, D.Y. Goswami, A review of the mechanisms and modeling of photocatalytic disinfection, Appl. Catal. B: Environ. 98 (2010) 27–38.

[182] Q. Li, S. Mahendra, D.Y. Lyon, L. Brunet, M.V. Liga, D. Li, P.J.J. Alvarez, Antimicrobial nanomaterials for water disinfection and microbial control: Potential applications and implications, Water Res. 42 (2008) 4591–4602.

[183] K. Page, R.G. Palgrave, I.P. Parkin, M. Wilson, S.L.P. Savin, A.V. Chadwick, Titania and silver-titania composite films on glass-potent antimicrobial coatings, J. Mater. Chem. 17(1) (2007) 95–104.

[184] J.P. Kim, I.H. Cho, I.T. Kim, C.U. Kim, N.H. Heo, S.H. Suh, Manufacturing of anti-viral inorganic materials from colloidal silver and titanium oxide, Rev. Roum. Chim. 51(11) (2006) 1121–2911.

[185] S.B. Atla, C.-C. Chen, C.-Y. Chen, P.-Y. Lin, W. Pan, K.-C. Cheng, Y.M. Huang, Y.-F. Chang, J.-S. Jean, Visible light response of $Ag^+/TiO_2–Ti_2O_3$ prepared by photodeposition under foam fractionation, J. Photochem. Photobiol. A: Chem. 236 (2012) 1–8.

[186] W. Wang, L. Zhang, T. Anc, G. Li, H.-Y. Yip, P.-K. Wong, Comparative study of visible-light-driven photocatalytic mechanisms of dye decolorization and bacterial disinfection by B-Ni-codoped TiO_2 microspheres: The role of different reactive species, Appl. Catal. B: Environ. 108–109 (2011) 108–116.

[187] A.G. Agrios, P. Pichat, State of the art and perspectives on materials and applications of photocatalysis over TiO_2, J. Appl. Electrochem. 35 (2005) 655–663.

[188] P. Wu, R. Xie, K. Imlay, J.K. Shang, The antibacterial action of nanocrystalline ZnS is compared with Evonik-Degussa P-25, Environ. Sci. Technol. 44 (2010) 6992–6997.

[189] D.W. Synnott, M.K. Seery, S.J. Hinder, G. Michlits, S.C. Pillai, Anti-bacterial activity of indoor-light activated photocatalysts, Appl. Catal. B: Environ. 130–131 (2013) 106–111.

[190] T.N. Obee, R.T. Brown, TiO_2 Photocatalysis for indoor air applications: Effects of humidity and trace contaminant levels on the oxidation rates of formaldehyde, toluene, and 1,3-butadiene, Environ. Sci. Technol. 29 (1995) 1223–1231.

[191] P. Chin, L.P. Yang, D.F. Ollis, Formaldehyde removal from air via a rotating adsorbent combined with a photocatalyst reactor: Kinetic modelling, J. Catal. 237 (2006) 29–37.

[192] T. Tsuru, T. Kan-no, T. Yoshioka, M. Asaeda, A photocatalytic membrane reactor for VOC decomposition using Pt-modified titanium oxide porous membranes, J. Membr. Sci. 280 (2006) 156–162.

[193] C.H. Ao, S.C. Lee, Indoor air purification by photocatalyst TiO_2 immobilized on an activated carbon filter installed in an air cleaner, Chem. Eng. Sci. 60 (2005) 103–109.

[194] H. Ichiura, T. Kitaoka, H. Tanaka, Photocatalytic oxidation of NO_x using composite sheets containing TiO_2 and a metal compound, Chemosphere 51 (2003) 855–860.

[195] M. Kitano, M. Matsuoka, M. Ueshima, M. Anpo, Recent developments in titanium oxide-based photocatalysts, Appl. Catal. A: Gen. 325 (2007) 1–14.

[196] L. Wang, Paving out pollution, Scientific American, Feb. 23 (2002).

[197] D. Jung, G. Kim, M.-S. Kim, B.-W. Kim, Evaluation of photocatalytic activity of carbon-doped TiO_2 films under solar irradiation, Korean J. Chem. Eng. 29(6) (2012) 703–706.

[198] D. Li, Z. Chen, Y. Chen, W. Li, H. Huang, Y. He, X. Fu, A new route for degradation of volatile organic compounds under visible light: Using the bifunctional photocatalyst $Pt/TiO_{2-x}N_x$ in $H_2–O_2$ atmosphere, Environ. Sci. Technol. 42 (2008) 2130–2135.

[199] Z. Wei, J. Sun, Z. Xie, M. Liang, S. Chen, Removal of gaseous toluene by the combination of photocatalytic oxidation under complex light irradiation of UV and visible light and biological process, J. Hazard. Mater. 177 (2010) 814–821.

[200] J. Nowotny, C.C. Sorrell, L.R. Sheppard, T. Bak, Solar-hydrogen: Environmentally safe fuel for the future, Int. J. Hydrogen Energy 30 (2005) 521–544.

[201] M. Matsuoka, M. Kitano, M. Takeuchi, K. Tsujimaru, M. Anpo, J.M. Thomas, Photocatalysis for new energy production: Recent advances in photocatalytic water splitting reactions for hydrogen production, Catal. Today 122 (2007) 51–61.

[202] A.L. Linsebigler, G. Lu, J.T. Yates, Photocatalysis on TiO_2 surfaces: Principles, mechanisms, and selected results, Chem. Rev. 95 (1995) 735–758.

[203] S.G. Yan, J.T. Hupp, Semiconductor-based interfacial electron-transfer reactivity: Decoupling kinetics from pH-dependent band energetics in a dye-sensitized titanium dioxide/aqueous solution system, J. Phys. Chem. 100 (1996) 6867–6870.

[204] T. Hannappel, B. Burfeindt, W. Storck, Measurement of ultrafast photoinduced electron transfer from chemically anchored Ru-dye molecules into empty electronic states in a colloidal anatase TiO_2 film, J. Phys. Chem. B 101 (1997) 6799–6802.

[205] I. Martini, J.H. Hodak, G.V. Hartland, Effect of water on the electron transfer dynamics of 9-anthracenecarboxylic acid bound to TiO_2 nanoparticles: demonstration of the Marcus inverted region, J. Phys. Chem. B 102 (1998) 607–614.

[206] B. Burfeindt, T. Hannappel, W. Storck, F. Willig, Measurement of temperature-independent femtosecond interfacial electron transfer from an anchored molecular electron donor to a semiconductor as acceptor, J. Phys. Chem. 100 (1996) 16461–16465.

[207] J.M. Rehm, G.L. Mclendon, Y. Nagasawa, K. Yoshihara, J. Moser, M. Gratzel, Femtosecond electron-transfer dynamics at a sensitizing dye-semiconductor (TiO_2) interface, J. Phys. Chem. 100 (1996) 9577–9578.

[208] K.B. Dhanalakshmi, S. Latha, S. Anandan, P. Maruthamuthu, Dye sensitized hydrogen evolution from water, Int. J. Hydrogen Energy 26 (2001) 669–674.

[209] W.W. So, K.J. Kim, S.J. Moon, Photo-production of hydrogen over the $CdS–TiO_2$ nano-composite particulate films treated with $TiCl_4$, Int. J. Hydrogen Energy 29 (2004) 229–234.

[210] G.C. De, A.M. Roy, S.S. Bhattacharya, Effect of n-Si on the photocatalytic production of hydrogen by Pt-loaded CdS and CdS/ZnS catalyst, Int. J. Hydrogen Energy 21 (1996) 19–23.

[211] A. Koca, M. Sahin, Photocatalytic hydrogen production by direct sun light from sulfide/sulfite solution, Int. J. Hydrogen Energy 27 (2002) 363–367.